Defining Lignin Nanoparticle Properties through Tailored Lignin Reactivity by Sequential Organosolv Fragmentation Approach (SOFA)

Journal:	*Green Chemistry*
Manuscript ID	GC-ART-10-2018-003290
Article Type:	Paper
Date Submitted by the Author:	19-Oct-2018
Complete List of Authors:	Liu, Zhi-Hua; Texas A&M University, Hao, Naijia; State Key Laboratory of Fine Chemicals, Dalian University of Technology Shinde, Somnath; University of Tennessee Knoxville, Chemical and Biomolecular Engineering Pu, Yunqiao; Oak Ridge National Laboratory, Kang, Xiaofeng; Texas A&M University Ragauskas, Arthur; University of Tennessee, Yuan, Joshua; Texas A&M University, Institute for Plant Genomics and Biotech

Defining Lignin Nanoparticle Properties through Tailored Lignin Reactivity by Sequential Organosolv Fragmentation Approach (SOFA)

Zhi-Hua Liu [a,b], Naijia Hao [c], Somnath Shinde [c], Yunqiao Pu [d], Xiaofeng Kang [e], Arthur J. Ragauskas [c, d, f], Joshua S. Yuan [a,b,*]

[a] Synthetic and Systems Biology Innovation Hub (SSBiH), Texas A&M University, College Station, TX 77843, USA

[b] Department of Plant Pathology and Microbiology, Texas A&M University, College Station, TX 77843, USA

[c] Department of Chemical & Biomolecular Engineering, University of Tennessee, Knoxville, TN 37996, USA

[d] Biosciences Division, Oak Ridge National Laboratory, Oak Ridge, TN 37830, USA

[e] Department of Molecular & Cellular Medicine, Texas A&M University, College Station, TX 77843, USA

[f] Joint Institute of Biological Sciences, Biosciences Division, Oak Ridge National Laboratory, Oak Ridge, TN 37831, USA

*Corresponding contributor. E-mail: *syuan@tamu.edu*

Abstract

Sustainable biorefinery heavily depends on the generation of value-added products, particularly from lignin. Despite most efforts, the production of fungible lignin bioproducts is still hindered by poor fractionation and low reactivity of lignin. To address these challenges, sequential organosolv fragmentation approach (SOFA) using ethanol plus different-stage catalysts was explored to selectively dissolve lignin to produce multiple uniform lignin streams, and tailor its chemistry and reactivity to fabricate lignin nanoparticles (LNPs) with desired quality features. In a biorefinery concept, the carbohydrate output was taken into consideration. SOFA significantly increased the glucose and xylose yield, suggesting an improved monomer-sugar release. The fractionated lignin was used to fabricate LNPs via self-assembly. Although these LNPs were derived from the same substrate, they exhibited different properties. The effective diameter almost followed the order of stage 1, stage 3, and stage 2 in each SOFA, and the smallest effective diameter was approximately 130 nm from SOFA using ethanol plus sulfuric acid. The polydispersity index and zeta potential were less than 0.08 and -50 mV, respectively, suggesting the good uniformity and stability of the LNPs. Lignin characterization results suggested that SOFA using ethanol plus sulfuric acid produced high-molecular-weight lignin, decreased the S/G ratio, β-O-4 and β-β linkage abundance, yet produced the condensed lignin and enhanced its hydrophobicity. More importantly, it exposed more phenolic OH groups and enhanced the stability of LNPs likely due to the hydrogen bond network. Together with enriched COOH group, it promoted the formation of electrical double layers and increased the zeta potential of LNPs. As a result, by tailoring the lignin chemistry using SOFA to enhance the self-assembling process, high-quality LNPs with a spherical shape, small effective diameter, and good stability have been fabricated, which represents a sustainable mean for upgrading the low-value lignin and thus contributes to the profitability of biorefineries.

Keywords: Sequential organosolv fragmentation approach (SOFA); lignin reactivity; lignin nanoparticles (LNPs); lignin reactivity; carbohydrate output

1 Introduction

Lignocellulosic biomass (LCB) represents an abundant and renewable resource to produce fuels, chemicals, and materials to substitute for fossil fuel usage. LCB has a complex architecture formed from three main classes of biopolymers: cellulose, hemicellulose, and lignin. The key to achieving a sustainable biorefineries depends on the fractionation of these polymers to usable platform molecules to produce a series of value-added products [1-3]. In conversional biorefineries, first and foremost, the carbohydrates are converted into biofuels [4-6]. Lignin, the second most abundant natural polymer after cellulose, is typically underused [7, 8]. Improvements in lignin valorization are essential for sustainable biorefineries based on economic and environmental analyses [3, 9, 10]. Despite most efforts, the production of fungible lignin products is uneconomic due to the poor fractionation and low reactivity of lignin. It is still unclear how fractionation technologies tailor lignin chemistry and reactivity and how the tailored chemistry defines the properties of lignin-derived product.

From the evolutionary perspective, the chemistry of lignin is crucial to its roles in the rigidity of plants and the transport of water. Lignin is a complex alkyl-aromatic biopolymer synthesized from three monolignol units: *p*-hydroxyphenyl (H), guaiacyl (G) and syringyl (S) units via radical coupling reactions with various interunit linkages, such as β-O-4, β-5, β-β, etc. Generally, the monolignol units contains various functional groups, including hydroxyl, carbonyl, and methoxyl groups [11, 12]. The amount and distributions of lignin varies with species, tissues, and cell wall structure in plant [13, 14]. Generally, the lignin concentration is higher in the middle lamellar and cell corners than in the secondary wall [13, 15]. However, the secondary wall occupies a larger portion of the wall and has the highest lignin content. The phenylpropanoid unit, interunit linkages, and functional groups, are also dependent on plant species, tissues, and cell wall structure [16]. Grasses are derived from three phenylpropanoid monomers. However, softwood lignin is almost exclusively derived from coniferyl alcohol (~95%) with ~5% coumaryl alcohol, while the predominant unit of hardwood lignin is sinapyl alcohol (45~75%), followed by coniferyl alcohol

(25~50%). Lignin in fibers is enriched in S units, whereas lignin in vessels is enriched in G units [13]. In the middle lamellar and the primary wall, lignin forms spherical structures, while in the secondary wall, lignin forms lamellae that follow the microfibrils orientation [15, 17]. Overall, lignin is a highly heterogeneous polymer, and its distribution and chemical properties depend on the cell wall structure.

Despite its heterogeneous structure of lignin itself, lignin acts like a 'resin' by cross-linking with carbohydrates to form lignin-carbohydrate complex (LCC), which further confers resistance toward chemico-biological attack [18, 19]. The complete utilization of the entire LCB is difficult in conversional biorefineries due to the complex lignin structure and the LCC, which prevent the cost-competitive fractionation of three polymers. Additionally, the inherent value of LCB highly depends on the ability to fractionate lignin polymer, and rather than just exploit the more uniform carbohydrates [4, 20, 21]. Current challenges in lignin valorization lie in poor fractionation efficiency and its low reactivity, as mentioned above, which is sensitive to its molecular weights, unit types, chemical linkages, and functional groups [3, 22]. Pretreatment and/or fractionation could determine the depolymerization of lignin to generate more uniform molecules with a high reactivity and thus improve the propensity for subsequent valorization. Lignin solubilization should be 'heterogeneous' kinetic model due to its inherent polydispersity. Fractionation may result in the irreversible dissolution of different lignin fragments or molecules, which react at different rates with the further progress of delignification [23, 24]. Another heterogeneous delignification kinetic model has been confirmed to consist of a faster or dominant one and a residual slower one [25]. Wang et al. also found that the dissolution rate of lignin in the secondary wall regions was faster than that in cell corner middle lamella regions [26]. Therefore, the dissolution and reactivity of lignin exhibit various behaviors in different fractionation phases and significantly depend on the plant species, cell wall structure, and fractionation employed.

Despite the challenges in processing, lignin represents a unique new feedstock in the formation of functional materials, such as nanoparticles. The use of many synthetic inorganic nanoparticles leads to a long-term environmental influence due to

the possible resistance to degradation [27, 28]. Because of its origin, lignin possesses numerous eco-friendly properties, such as biodegradability, biocompatibility, and low toxicity. Due to these advantages, technical lignin has been valorized to produce environmentally friendly lignin nanoparticles (LNPs), which have been considered as a promising alternative approach for lignin valorization to address challenges in the fields of environmental remediation, food and agriculture, and health care [26, 28-30]. Despite the progress, a number of technical challenges are yet to be addressed to improve lignin properties for LNPs. First and foremost, it is necessary to understand in-depth the impaction of fractionation on lignin chemistry and reactivity. It is also crucial to systematically understand the structure-activity-function relationships between lignin and LNPs for the sustainable valorization. In particular, it is important to reveal how the technical lignin chemistry, such as the hydrophilicity of functional groups, the molecular weights, and the type and amount of linkages, can define the size distribution, morphology, and stability of LNPs, all of which further define the LNP functions for extensive applications. Thus, application of the knowledge to design new fractionation is in turn critical to generate functional lignin with specific reactivity to be used for LNP fabrication. Unfortunately, a lack of knowledge of how lignin chemistry is modified by fractionation employed and what key factors define the LNPs properties hinder the development of well-designed fractionation as well as high-quality LNPs, making the lignin valorization through LNPs highly challenging.

To address these problems, sequential organosolv fragmentation approach (SOFA) was developed to overcome the lignin heterogeneity by selectively dissolving lignin to produce multiple uniform lignin streams with specific reactivities, which may be suitable for the fabrication of high-quality LNPs. Several SOFAs were evaluated to deconstruct corn stover, fractionate the lignin, and tailor its chemistry. In a biorefinery concept, enzymatic hydrolysis was conducted to build the sugar platform to assess the SOFA efficiency by synergistically improving carbohydrate output. Lignins from each SOFA were used to fabricate LNPs. The morphology, size distribution, charge, and stability of LNPs were characterized to define their performance. 2D- HSQC, and ^{31}P-NMR analyses were employed to characterize the lignin chemistries and their

correlations with the LNP properties. Overall, this study has the potential to reveal the lignin chemistry tailored by SOFA, the key factors that affected the LNP fabrication, and the structure-activity function relationships between lignin and LNPs.

2 Materials and Methods

2.1 Sequential organosolv fragmentation approach (SOFA) of corn stover

Corn stover was harvested from the suburb of Comanche, Texas, United States. Sequential organosolv fragmentation approach (SOFA) of corn stover was designed and evaluated using low holding temperature towards improving carbohydrate release and tuning lignin reactivity for LNP fabrication (Table 1). The schematic process of SOFA was presented in Figure 1.

To remove the non-structural components (e.g. water extractives and ash) and purify lignin stream, corn stover was first pre-washed using liquid hot water at 120°C for 30 min. After pre-washing, 50 g washed corn stover (dry weight, dw) was loaded into a 1.0 l screw bottle at 10% (w/w) solid loading. During SOFA, 50% ethanol solution with 1% dilute sulfuric acid (SA), 2% formic acid (FA), or 1% sodium hydroxide (SH) was employed to fragmentize corn stover in stage 1 for 15 min at 120 °C heating by Amsco® LG 250 Laboratory Steam Sterilizer (Steris, USA). The pretreated slurry from stage 1 was then filtered to separate solid fraction from liquid stream. The solid fractions were then fragmentized in stage 2 at 120 °C for 30 min, followed by stage 3 for 60 min. The fractionation of corn stover was sequentially conducted using organosolv solvent with an intermittent mode, which was named sequential organosolv fragmentation approach (SOFA).

Log R_0 is generally used to assess the pretreatment severity [29]:

$$\log R_0 = t \times \exp\left[(T - T_b)/\omega\right] \quad (1)$$

Where t is the residence time, min; T is the holding temperature, °C; T_b is the base temperature, 100 °C; ω is the fitted value based on the activation energy, 14.75.

The combined severity factor log R_0" has been employed to assess the severity of SOFA as different solvents were used in the fragmentation of corn stover [30].

$$\log R_0'' = \log R_0 + |\mathrm{pH}-7| \quad (2)$$

2.2 Enzymatic hydrolysis of solid fraction

The solid fraction from SOFA was enzymatically hydrolyzed by Cellic CTec2 and HTec 2. Filter paper activity (FPU) of Cellic CTec2 is 96 FPU/ml, and the cellobiase activity is 1270 CBU/ml. Each hydrolysis assay was conducted in a 250 ml Erlenmeyer flask with 100 g of total mixture at pH 4.8 (5 mM citrate buffer), 50 °C, and 200 rpm for 168 h. The cellulase loading of 15 FPU/g solid and the volumetric ratio of CTec2:HTec2 10:1 were used. The solid loading was 3.0%. Sugar conversion was calculated from the ratio of sugar released from solid fraction used in hydrolysis.

2.3 Self-assembly fabrication of lignin nanoparticles (LNPs)

To prepare LNPs, the liquid stream containing fractionated lignin from each SOFA was filtered with a 0.22 μm filter membrane and acidified to a pH 2.0 with concentrated HCl to precipitate lignin. The lignin precipitates were collected in tared centrifuge tubes by centrifugation at 10000 rpm for 15 min, washed using ddH_2O, and then freeze-dried in a lyophilizer at -55 °C for 24 h (Labconco Corporation, USA). The fractionated lignin without post chemical modification was used to fabricate the LNPs via self-assembly. A modified preparation procedure of LNPs were employed [31, 32]. Lignin solubility is generally dependent on the fractionation methods and solvents employed, and lignin obtained from SOFAs is water-insoluble, but it can be dissolved into tetrahydrofuran. The freeze-dried lignin was thus dissolved in tetrahydrofuran at a concentration of 5 mg/ml. The mixtures were sonication treated for 30 min to make a pure solution. The solution was then filtered through a 0.45 μm syringe filter to remove undissolved particles, and rapidly loaded into a dialysis bag (Spectra/Por® 1 Dialysis Membrane Standard RC Tubing, 6-8 kDa, Spectrum Labs, USA). The dialysis bag was put into 50X volume deionized water with agitation speed of 50 rpm. During the dialysis, the deionized water was periodically replaced to remove tetrahydrofuran and form nanoparticle dispersion. The dispersion was used for microscopic analysis to determine the size, morphology, and charge of LNPs. The LNP pellet was collected by centrifuging the supernatant at 10,000 rpm for 30 min and dried at 65°C. The LNP yield was reported as gravimetric weight of the pellet using an analytical balance.

2.4 Characterizations of lignin nanoparticles (LNPs)

The particle size and zeta potential of the LNP dispersion was measured using a Brookhaven ZetaPlus Zeta Potential Analyzer, Brookhaven Instruments Corporation, New York, USA. Scanning electron microscopy (SEM) images of LNPs were obtained on a Zeiss Auriga 40 instrument with an acceleration voltage of 30 kV. Scanning transmission electron microscopy (STEM) images were obtained using an acceleration voltage of 30 kV.

2.5 Characterizations of the fractioned lignin

2.5.1 Cellulolytic enzyme lignin isolation from corn stover

Corn stover native lignin (CSNL) was isolated by cellulolytic enzyme [33]. The extractives-free corn stover was ball-milled using a planetary ball mill (Retsch PM 100) with zirconium dioxide vessels containing ZrO_2 ball bearings at 600 rpm for 2 h. The ball-milled sample was then hydrolyzed using 0.1 ml Cellic® CTec2/g solid and 0.1 ml Cellic® HTec2/g solid at 50 °C for 24 h. The hydrolysates were removed by centrifugation, and the solid residues were hydrolyzed again. The solid residues were treated with protease (Streptomyces, Sigma-Aldrich) to remove residual enzymes at 37 °C for 24 h, and then extracted by 96% dioxane. CSNL was recovered from the dioxane extracts using a rotary evaporator, and freeze-dried for further analysis.

2.5.2 2D HSQC NMR analysis

The 2D- ^{1}H-^{13}C heteronuclear single quantum coherence (HSQC) nuclear magnetic resonance (NMR) spectra were obtained with a Varian 500 MHz NMR spectrometer with the "gradient HSQCAD" mode. 30~50 mg of the lignin was dissolved in 0.6 ml dimethylsulfoxide (DMSO)-d_6 for the analysis. The gradient-enhanced HSQC with adiabatic pulses (gHSQCAD) mode was employed. The parameters of the measurements are as follows: 1.0 pulse delay, 32 scans, 1024 data points for ^{1}H, 256 increments for ^{13}C. The ^{1}H and ^{13}C spectral widths are 13.0 and 220.0 ppm, respectively. The central solvent peak (δC/δH=39.5/2.49 ppm) was used for reference. The data processing was conducted using Mestrenova software.

2.5.3 ^{31}P NMR analysis

The ^{31}P NMR spectra of lignin samples were acquired according to the published methods [34]. In detail, 20-25 mg lignin sample was dissolved in 0.7 ml stock solution

of pyridine/$CDCl_3$ (v/v = 1.6/1) including 1.25 mg/ml $Cr(acac)_3$ and 2.5 mg/ml internal standard *endo*-N-hydroxy-5-norbene-2,3-dicarboxylic acid imide (NHND). The vial was shaken until the lignin was dissolved completely. Prior to the analysis, 70 μl phosphorylating reagent 2-chloro-4,4,5,5-tetramethyl-1,3,2-dioxaphospholane (TMDP) was added to the vial and mixed well. Quantitative ^{31}P NMR spectra were acquired on a Bruker 500 MHz spectrometer using an inverse-gated decoupling pulse sequence, 90° pulse angle, 1.2 s acquisition time, 25 s pulse delay, and 64 scans.

2.5.4 Gel-permeation chromatography (GPC) analysis

The lignin was acetylated with acetic anhydride/pyridine (1/1, v/v) for 24 h in a sealed flask under an inert atmosphere. The lignin concentration was 2 mg/ml. After 24 h, the lignin solution was diluted with 20 ml of ethanol and stirred for 30 min. The solvents were removed with a rotary evaporator, and then the sample was dried in a vacuum oven at 40 °C. Prior to GPC analysis, the acetylated lignin was dissolved in tetrahydrofuran (1.0 mg/ml), filtered through a 0.45 μm filter. The molecular weight distributions of the acetylated lignin was then analyzed on an Agilent GPC SECurity 1200 system equipped with three Waters Styragel columns (HR1, HR2 and HR6), an Agilent refractive index (RI) detector, and an Agilent UV detector (270 nm), using tetrahydrofuran (THF) as the mobile phase (1.0 ml/min), with an injection volume of 20.0 μL. A standard polystyrene sample was used for calibration.

2.6 Sugar analysis methods

Composition analysis was carried out according to the Laboratory Analysis Protocol (LAP) of the National Renewable Energy Laboratory (NREL), Golden, CO, USA. The sugars were analyzed by Ultimate 3000 HPLC System (Thermo Scientific, USA) equipped with an Aminex HPX-87P carbohydrate analysis column (Bio-Rad Laboratories, CA) and a refractive index detector using HPLC grade water as the mobile phase at a flow rate of 0.5 ml/min. Error bars in the Tables and Figures represented the standard deviation of the replicates.

3 Results and Discussion

3.1 Component transformation in each SOFA

Component transformation is essential to evaluate the fractionation for the

techno-economic analyses [35, 36]. Component content in the solid fraction from each SOFA is given in electronic supplemental information A (ESI A). The results showed that component transformation was significantly dependent on the SOFA employed. The glucan content in the pretreated solid increased after each SOFA and obviously increased in the order of stage 1, stage 2, and stage 3, which were due to the removal of hemicelluloses, lignin, and other soluble components by fractionation [37, 38]. Interestingly, the xylan content was lowest in the pretreated solid from SOFA using ethanol plus sulfuric acid (ESA) compared to other SOFAs, suggesting the dissolution and degradation of xylan due to the acid hydrolysis effects [37, 39]. SOFA using ethanol plus formic acid (EFA) and ethanol removed less xylan from corn stover as compared to that using ESA due to the week acids employed. On the contrary, SOFA using ethanol plus sodium hydroxide (ESH) reserved more xylan as compared to others. As for lignin content, it decreased after SOFA using ESA and ESH and obviously decreased in the order of stage 1, stage 2, and stage 3, suggesting the effective removal of lignin by the combined effects of ethanol solvent and catalysts.

ESI B shows the enzymatic hydrolysis results of the solid fraction from SOFAs. SOFAs resulted in 2.4-6.5 and 3.7-8.7 times higher glucan and xylan conversion of pretreated solid than that of corn stover feedstock (CSFS), respectively. As expected, the glucan and xylan conversion increased in the order of stage 1, stage 2, and stage 3 in each SOFA, suggesting an improved hydrolysis efficiency at the later SOFA stages. SOFAs using ESA and ESH produced the highest sugar conversion at each stage compared to other SOFAs. Generally, the hydrolysis performance is closely related to the accessible surface area of carbohydrates to the enzymes [40, 41]. As confirmed by component transformation analysis (ESI A, C, and D), SOFA using ESA and ESH efficiently deconstructed corn stover and exposed more accessible carbohydrates surface area due to the removal of hemicelluloses and the dissolvation of lignin. SOFA using ESA at stage 3 removed more than 90% xylan and 70% lignin from corn stover, while SOFA using ESH dissolved more than 30% xylan and 80% lignin (ESI C), and together, they produced more than 96% glucan and 95% xylan conversion.

Sugar yield has been identified as one of the most crucial metrics to assess the

fractionation performance in a biorefinery concept. The monomer sugars released from carbohydrate were characterized to evaluate the SOFA performance for establishing the sugar platform (Figures 1 and 2). Results showed that the glucose and xylose yields also increased as the order: stage 1, stage 2, and stage 3 in each SOFA, suggesting an improved monomer sugar release at the later SOFA stages. SOFAs using ESA and ESH also produced higher yields of glucose and xylose at each stage compared to other SOFAs. The glucose yields from SOFA using ESA and ESH at stage 3 were 92% and 88%, respectively, while the xylose yields were 77% and 84%. SOFAs with ESA and ESH led to more monomer sugar release likely due to better deconstruction performance of corn stover. Overall, SOFAs with ESA and ESH, especially at the later stages, improved the hydrolysis performance by dissolving the xylan and lignin and thus transferred more carbohydrates into the monomer sugar, which facilitated the production of biofuels and value-added products.

3.2 Lignin transformation in the solid and liquid stream after SOFA

Lignin valorization is increasingly recognized as being crucial to the sustainable biorefineries [3, 20]. Depolymerization of lignin is an important starting point for its valorization because it could generate a source of low molecular-weight lignin oligomers and/or aromatics suitable for downstream processing. Since it is heterogeneous and exists in the different layers of the plant cell wall, lignin polymer may have different dissolving behaviors and properties. Here, we developed four SOFA configurations for lignin depolymerization to yield multiple soluble uniform lignin streams for high-value utilization. Specifically, SOFAs employing ethanol and either sulfuric acid, formic acid, or sodium hydroxide as catalyst at three stages were evaluated to sequentially depolymerize lignin. The heterogeneous lignin polymer should have different dissolving behaviors at each stage of SOFA and thus possessed its specific reactivity suitable for the preparation of functional products.

The substantiality of lignin valorization emphasizes on the lignin release from biomass [4, 42]. Figure 3 shows the lignin distribution in the solid and liquid streams after each SOFA. SOFAs using ESA and ESH effectively depolymerized lignin polymer and thus fractionated more lignin into the liquid stream at each stage

compared to other SOFAs. SOFA using ESA broke the lignin-carbohydrate linkages, caused lignin to coalesce into larger molten bodies that migrated within and out of the cell wall, and then dissolved lignin into polar ethanol solution [43-45]. SOFA using ESH broke the ester and glycosidic side chains and caused the cleavage of phenolic alkyl-aryl ethers by nucleophilic cleavage, promoting lignin solvation [46, 47]. Interestingly, the soluble lignin yield in the liquid stream was the highest at stage 1 in each SOFA and showed diminishing values at stages 2 and 3. For example, the soluble lignin yield was 42%, 20% and 16% at stages 1, 2 and 3 for SOFA using ESA and 48%, 16% and 17% for SOFA using ESH, respectively. These results highlighted that SOFA using ESA and ESH at stage 1 generated more soluble lignin, which could be classified as an easily dissolved lignin. Lignin fractionated at stages 2 and 3 could be classified as an ordinarily dissolved lignin. Using the three stages of SOFAs with ESA and ESH, more than 78% and 81% of total lignin were dissolved into the liquid stream, suggesting the high fractionation efficiency of SOFA. After SOFAs using ESA and ESH, 23% and 19% lignin were still retained in the solid fraction, respectively, which could be classified as hard-dissolved lignin. Overall, lignin polymer showed different dissolving behaviors at the three stages of SOFA. SOFAs using ESA and ESH generated more easily dissolved lignin at stage 1 and more ordinary dissolved lignin at stages 2 and 3 compared to other SOFAs.

3.3 Self-assembly fabrication of lignin nanoparticles (LNPs)

The amphiphilic lignin fractionated at each stage of SOFA using ESA and ESH was used to fabricate LNPs via self-assembly. Figure 4 and ESI E show the particle size distributions and the images of LNPs, respectively. The morphology and particle size distributions were observed to be dependent on the fragmentation approach employed. LNPs exhibited a spherical structure, and they obtained from SOFA using ESA had smaller particle size and more symmetric and uniform round shape than that using ESH. The LNP yield was 78.8%, 77.6%, 73.4% at stages 1, 2, 3 for SOFA using ESA and 67.0%, 66.0%, 62.6% for SOFA using ESH, respectively, suggesting that the LNP yield was also dependent on the fragmentation approach employed (ESI F).

Figure 5 shows that the properties of LNPs were also dependent on the SOFA

employed. An effective diameter of LNPs is a key metric for assessing their properties and the applications. The effective diameter of LNPs from SOFA using ESA followed the order stage 1 (132 nm) < stage 3 (473 nm) < stage 2 (581 nm), while it followed the order stage 3 (693 nm) < stage 1 (807 nm) < stage 2 (1099 nm) from SOFA using ESH. The largest one was obtained at stage 2 for both SOFAs, while the smallest one was obtained at stage 1 using ESA and at stage 3 using ESH, respectively, indicating that SOFA determined the effective diameter. Interestingly, SOFA using ESA produced a smaller effective diameter of LNPs compared to that using ESH at each stage. The particle size distribution of LNPs was fitted by Gaussian function and the half-width of the fitting peak was used to evaluate the uniformity of LNPs. Results showed that the half-width for SOFA using ESA (less than 50 nm) was lower than that using ESH. Polydispersity index (PDI) is another factor used for assessing the uniformity of particles. The PDI was less than 0.08 for all LNPs, and the PDI from SOFA using ESA at each stage was also lower than that using ESH. A previous study reported that the PDI of LNPs from dissolved lignin by *p*-toluenesulfonic acid (*p*-TsOH) fractionation was 0.163-0.184 [48]. Generally, lower PDI indicated lower polydisperse. These results suggested that LNPs prepared from the fractionated lignin by SOFA especially using ESA were more uniform.

Zeta potential of particles determines the stability of emulsions. Figure 5 shows that LNPs had negative values of zeta potential, which was partially due to the true negative charges of the phenol groups in lignin and partially due to the adsorption of hydroxyl ions on the hydrophobic surface of lignin [28, 31, 49]. The negative surface charge can electrostatically stabilize the LNPs and thus prevent their aggregation. The zeta potentials of LNPs from SOFA using ESA followed the order stage 2 (-49.2 mV), stage 1 (-56.1 mV), and stage 3 (-57.7 mV), while for SOFA using ESH, they followed the order stage 1 (-52.4 mV), stage 3 (-52.9 mV), and stage 2 (-58.4 mV). The LNPs from SOFA using ESA had higher zeta potential than those using ESH at stages 1 and 3. Generally, when the zeta potential is high in LNP dispersions, the repulsive forces exceed the attractive forces, resulting in a relatively stable system. The LNP dispersions with low absolute zeta potentials tend to coagulate, leading to

poor physical stability. Previous studies reported that the zeta potential of LNPs from dissolved lignin by *p*-TsOH was between -27.2 and -40.0 mV [1, 48]. The zeta potential of LNPs prepared from low-sulfonated lignin was approximately -40 mV [50]. Results suggested that LNPs from SOFA possessed higher zeta potential and thus physical stability. Taking these metrics into consideration, SOFAs using ESA at stage 1 and ESH at stage 3 produced more uniform and stable LNPs, respectively, due to relatively smaller particles sizes, lower PDIs, and higher zeta potentials. Therefore, SOFA employing different solvents and stages could give rise to multiple lignin streams to guide the fabrication of LNPs with specific properties.

3.4 Stability of LNPs at different storage periods, pH values and ionic strengths

The stability of LNPs under different conditions is crucial for their applications. The effects of conditions, such as storage period, pH value, and ionic strength, on the property of LNPs were evaluated. Figure 5 illustrates the storage period effects on the stability of LNPs. The effective diameter, PDI, and zeta potential of LNPs had hardly changed after 7-day storage, indicating the LNP stability in pure water. The long-term stability of LNPs particularly demonstrates a potential for the various applications.

The most important factor that affects the LNP stability is the pH of the aqueous dispersion. Figure 6 shows that the effects of pH on the properties of LNPs depended on the SOFA employed. The effective diameter from SOFA using ESA at pH 3.0 was 1.0 to 3.8 times higher than that under neutral conditions, suggesting the slightly aggregation of LNPs. Interestingly, the effective diameter from SOFA using ESH had hardly changed with varied pH. The half-width and PDI from both SOFAs at pH 3.0 were 0.3-3.3 and 0.8-7.2 times higher than that under neutral conditions, respectively, suggesting a slightly reduced uniformity at pH 3.0. Although the absolute value of the zeta potential at pH 3.0 decreased by 29-57% compared to that under neutral conditions, it was still between -23 mV and -35 mV. A similar trend of the zeta potential of LNPs prepared from Kraft lignin with pH variation was observed in previous reports [31, 49, 51], which showed that the protonation of charged groups below pH 4.0 resulted in a drastic decrease in zeta potential. When the pH value increased from a neutral value to 11.0, the effective diameter from SOFA using ESH had hardly

changed, suggesting no aggregation or dissolution of LNPs, while the effective diameter from SOFA using ESA increased. The half-width and PDI increased at pH 11.0, suggesting a slightly reduced uniformity. This phenomena is likely due to that LNPs start to disassemble toward dissolution under alkaline condition [49]. Interestingly, the absolute value of zeta potential at pH 11.0 increased by 16-60% compared to that under neutral conditions, and it reached -90 mV from SOFA using ESA at stage 1. A previous study also reported that the zeta potential of LNPs prepared from alkaline lignin reached -91.5 mV at pH 11.0 [49, 52]. The effect of pH on the electrical double layer repulsion was likely due to the complex protonation and deprotonation of the hydroxyl groups at various pH levels [31, 49]. Overall, although the half width and PDI slightly increased with varied pH, considering the high absolute value of zeta potential, LNPs from SOFA showed high stability in a broad range of pH values.

Since the potential application of LNPs might cover a wide range of ionic strengths, the response of LNPs to the change in ionic strength was evaluated. Figure 7 shows that although the zeta potential decreased by 26-40% at 50 mM NaCl compared to the absence of salt, the effective diameter and half width had hardly changed. When the NaCl concentration increased to 500 mM, the effective diameter, half-width, and PDI increased, and the zeta potential was close to 0 mV, suggesting the aggregation of the LNPs. Previous studies also reported the aggregation of LNPs and the reduction of zeta potential with the increase in salt concentration [31]. This phenomenon can be explained by the classical Derjaguin-Landau-Verwey-Overbeek (DLVO) theory of colloid stability. The balance between an electrostatic repulsion and a van der Waals attraction determines the LNP stability. Generally, the electrostatic repulsion becomes significant as two particles approach each other, and their electrical double-layers begin to interfere. The increase in salt concentration will reduce the range of double-layer repulsion between particles. As a result, the van der Waals attraction dominates the forces between particles and may eventually lead to the aggregation of LNPs. The decrease in the zeta potential is mainly due to the accumulation of Na^+ counter-ions around the LNPs and the consequent reduction in the thickness of the electrical double layer. Taken together, these results suggested that

LNPs from SOFA still possessed high stability over a broad range of ionic strength.

3.5 Tailored lignin reactivity by SOFA impacting LNP properties

It was interesting that although the LNPs were derived from the same corn stover substrate, they exhibited different properties. A greater understanding of lignin chemistry could help to reveal the fundamental mechanisms and thus provide important information to illuminate the formation of LNPs. Therefore, several techniques were employed to better understand the tailored chemical structures of lignin fractionated by SOFA, which enables a systemic investigation of relationship between lignin chemistry and LNP properties from several perspectives.

The weight-average molecular weight (M_w) and the number-average molecular weight (M_n) of lignin fractionated by SOFA was shown to impact LNP formation and diameters (Figure 8) [53]. Corn stover native lignin (CSNL) exhibited a M_n of 1371 g/mol and M_w of 6241 g/mol. Figure 8 demonstrated a varying phase in an obvious increase of M_n at stage 1, and M_n and M_w at stage 3 for SOFA using ESA and an almost unvarying phase of lignin M_n for SOFA using EFA and only ethanol. Previous studies have demonstrated the competition between lignin depolymerization and repolymerization under acidic conditions [54-56]. A gradual increase in molecular weight of lignin was observed with increasing severity of steam explosion, suggesting the simultaneous depolymerization by the cleavage of β-O-4 linked structures and repolymerization by acid-catalyzed condensation on the aromatics [54]. A similar effect in organosolv lignin extracted from *Miscanthus* was reported [55]. Increased pretreatment severity led to an increase in molecular weight of lignin, indicating the repolymerization reaction [55]. As a result, a carbonium ion may lead to an increase in the heterogeneity of the fractionated lignin and thus affect its solubility and reactivity. However, Tian et al. compared three cellulolytic enzyme lignins from steam-pretreated agriculture reside corn stover, hardwood poplar, and softwood lodgepole pine for LNPs and found the condensed lignin from steam explosion could potentially facilitate the formation of LNPs [49]. Figure 8 also demonstrated an obvious varying phase in a decrease of lignin Mn and Mw for all SOFAs, except the aforementioned ones, suggesting the deploymerization of lignin by these SOFAs,

especially using ESH. The decrease in lignin molecular weight is likely due to the nucleophilic cleavage of phenolic alkyl-aryl ethers under alkaline conditions [57, 58]. As compared to CSNL, most of the lignin fractions from SOFA have decreased PDI, suggesting that SOFA produced more uniform lignin and should facilitate the fabrication of LNPs [59]. Results showed that SOFA using ESA produced a higher molecular weight than that using ESH, which correlated with the fact that the LNPs from SOFA using ESA possessed a lower effective diameter. Additionally, the molecular weight of lignin was significantly dependent on the stage employed in SOFA. The M_n of lignin from SOFA using ESA was lower at stage 2 than that at stages 1 and 3, which almost showed an opposite trend to the effective diameter of LNPs. The M_w of lignin from SOFA using ESA was the highest at stage 3, followed by stage 2 and stage 1. For SOFA using ESH, the M_n and M_w was also lower at stage 2 as compared to stages 1 and 3, which showed an opposite trend to the effective diameter. PDI of the fractioned lignin was higher at stage 2 than stages 1 and 3 for SOFA using ESA, and it increased in the order stage 1, stage 2, and then stage 3 for that using ESH, which almost showed a similar trend as that of effective diameter. All these results suggested that the high-molecular-weight lignin with low PDI should be helpful in obtaining smaller effective diameters of LNPs.

The lignin reactivity also depends on the relative abundance of *p*-hydroxyphenyl (H), guaiacyl (G), and syringyl (S) units due to their different functional groups and chemical properties. Figure 9 and ESI G show that the three types of lignin had different dissolving behaviors at different SOFA stages. Compared with CSNL, SOFA using ESA fractionated more G- and H-type lignin while SOFA using ESH dissolved more S- and H-type lignin. SOFA using EFA and only ethanol led to minor changes on the S- and G-type lignin, but they enriched the H-type lignin. As a result, SOFA using ESA significantly decreased the S/G ratio, while SOFA using ESH increased the S/G ratio. Cao et al. found that in dilute acid pretreatment of *Populus trichocarpa*, the lignin S/G ratio was decreased with a longer residence time, which were accompanied with an increase in condensed lignin as evidenced by an increase in the content of aromatic carbon-carbon structures and a decrease in the number of protonated

aromatics [60]. The higher contents of S- and H-type lignin from steam-exploded corn stover and hardwood poplar could account for an increased particle size of LNPs [49], suggesting that enriched S- and H- type lignin may produce bigger LNPs. Regarding the specific stage, the S/G ratio from SOFA using ESA were slightly lower at stage 2 than stages 1 and 3, while the G-type lignin content was higher at stage 2 than stages 1 and 3. After SOFA using ESH, the S/G ratio followed the order stage 2 < stage 3 < stage 1. Results showed a clear correlation of the lignin units with the effective diameter of LNPs for the specific stage of SOFA. Lignin with lower S/G ratio and higher G-unit content from SOFA using ESA led to lower effective diameter of LNPs.

Figure 10 shows the lignin interunit linkages in CSNL and lignin produced after each SOFA, and the linkage abundance also impacted the LNP properties. Compared to CSNL, the β-O-4 and β-β linkage contents for lignin fractions out of SOFA were significantly decreased, while the β-5 linkage content depended on the stage and catalyst of the SOFA employed. Interestingly, SOFA using ESA broke down more β-O-4 and β-β linkage groups, while SOFA using ESH decreased more β-5 linkage group. These results suggested that SOFA significantly reduced the interunit linkages through the cleavage of β-O-4, β-β, and β-5 linkage groups, and thus depolymerized the lignin polymer. Previous study showed that during organosolv treatment of Loblolly pine, acid-catalyzed cleavage of β-O-4 linkages and ester bonds were the major mechanisms of lignin cleavage. This degradative pathway results in the formation of a dissolved and more condensed ethanol organosolv lignin [61]. Additionally, an increase in the degree of lignin condensation was observed in acid pretreatment, accompanying by a decrease in β-O-4 linkages, which were cleaved and recondensed during the acid-catalyzed reactions [62]. Results also suggested more cleavage of β-O-4 and β-β linkages with the increased lignin molecular weight also suggested the generation of condensed lignin by SOFA using ESA. For the specific SOFAs, the β-O-4 linkage group was lower at stage 2 than that at stages 1 and 3, which showed an opposite trend to the effective diameter of LNPs. These results indicated that the condensation of lignin from SOFA using ESA may occur as confirmed by higher content of β-5 linkages and higher molecular weight of lignin [54,

[63]. Previous studies reported that various extents of lignin condensation were accompanied by the cleavage of β-O-4 linkage groups in steam pretreatment, these condensed structures was favorable to the small-size LNPs formulation, which had a negative correlation with the β-O-4 linkage group [49].

SOFA also produced lignin fractions with diverse functional groups, which could impact the stability of LNPs. Specifically, the electrical-double layer repulsion resulting from the hydroxyl and carboxyl groups were likely to be the main drivers for stabilizing LNPs. Thus, the phenolic functional substructures of lignin produced from each SOFA have been quantified by ^{31}P NMR (Figure 11 and ESI H). As the contents and locations of the hydroxyl groups in these lignins were compared, it was apparent that lignin produced from SOFA using ESA indeed had more total phenolic OH groups compared to that using ESH, EFA and only ethanol. SOFA using ESA employed a much more aggressive extraction solvent, ethanol solution and sulfuric acid as the catalyst, which tended to extensively cleave the β-O-4 linkages as confirmed by 2D-NMR results, forming a large amount of free phenolic OH groups. The acid-catalyzed reaction between aromatics and free radicals by SOFA using ESA resulted in 10-45% increase in C5-substituted OH content, as compared to that using ESH, suggesting the formation of condensed lignin [56, 64]. The result was consistent with the interunit linkage and molecular weight data. Moxley et al. found that dilute acid pretreatment of corn stover significantly increases the total phenolic hydroxyl groups likely due to the cleavage of the aryl ether lignin bonds, and increases the carboxylic moieties in the isolated lignins partially due to the cleavage of the ester bonds from lignin-carbohydrate complexes [63]. The increased phenolic OH content in lignin may also enhance the stability of LNPs through intramolecular hydrogen bonding networks as the lignin's planar phenol groups may be densely packed in layer within the LNPs. In contrast, lignin fractionated by SOFA using ESH likely underwent less condensation but more fragmentation to result in a slight higher content of phenolic OH groups and 5.1-6.6 times higher content of COOH groups. Wang et al. also found that the content of total phenolic OH was elevated after the hydrothermal and alkaline pretreatments (NaOH) of *Eucalyptus* [26]. Lignin produced

by SOFA using ESH had more hydrophilic groups such as COOH groups, which should enhance the interaction between the surface of LNPs and water and thus increase the effective diameter of LNPs, as confirmed by above results (Figures 5 and 12). Previous study reported that the introduction of hydroxymethyl groups in lignin and further condensation with diphenylmethane-bonds formation helped the LNPs formation [59]. In addition, the hydroxyl and carboxyl groups provide the LNPs with a surface charge and promote the formation of electrical double-layers, stabilizing the LNP dispersion [28, 31, 49]. Figures 11 and 12 show that SOFA using ESA and ESH enriched the total phenolic OH and COOH groups, and thus promoted the formation of electrical double layers and increased the zeta potential of LNPs (Figure 5).

For specific SOFAs, SOFA using ESA produced more phenolic OH at stage 1, followed by stages 3 and 2, which showed an opposite trend to the effective diameter of LNPs (Figure 12), which supported the aforementioned results. SOFA using ESH produced more phenolic OH at stage 1, followed by stages 2 and 3. For COOH group, SOFAs using ESA and ESH at stage 2 yielded higher COOH content than that at stages 1 and 3, which showed a similar trend to the effective diameter (Figure 12). These results suggested that higher content of total phenolic OH and lower content of COOH group may not only enable the resulting LNPs with high solubility but also provide strong interactions between the LNPs and facilitate the fabrication of LNPs with smaller effective diameter. Overall, the formation of high-quality LNPs should be significantly defined by the synergistic effects of lignin chemistry tailored by SOFA, likely including increased molecular weight, decreased S/G ratio and β-O-4 linkage content, enriched phenolic OH and COOH groups (Figure 12).

3.6 Proposed formation mechanism of LNPs from lignin fractionated by SOFA

The formation mechanism of lignin LNPs should be different from that of conventional amphiphilic copolymers, as the current polymer colloid theory of random amphiphilic lignin has drawbacks reflecting its inherent heterogeneity [31, 32, 49]. In the present study, the amphiphilic lignin fractionated at each stage of SOFA using ESA and ESH was used as feedstock to fabricate LNPs. Tetrahydrofuran was employed to dissolve the lignin to form a pure solution. After sonication and filtration,

the pure solution was dialyzed to remove tetrahydrofuran. Lignin molecules associated with each other and then aggregated during the dialysis process. As a result, the spherical LNPs were obtained by gradual hydrophobic aggregation of lignin with different hydrophobic abilities in tetrahydrofuran and aqueous solutions. Lignin fractionated by SOFAs is an amphiphilic polymer, which is randomly formed from various hydrophobic phenylpropanoid units and some hydrophilic groups (hydroxyl and carboxyl groups) (Figures 8-11). Due to these properties, LNPs were probably formed in a phase separation process through a nucleation-growth, as the tetrahydrofuran was gradually replaced with water during dialysis. In particular, the hydrophobic aromatic skeletons of lignin aggregates in the water to form the cores of the LNPs, while the hydrophilic groups of lignin simultaneously form the shells of the LNPs [65]. The diverse chemistry of different lignin fractions from SOFAs allowed the thorough evaluation of several factors determining LNP formation.

First, the hydrophobic aromatic groups in lignin should be the main building units to form the cores of LNPs via non-bonded orbital interactions (π-π interaction) and van der Waals interactions. While the molecular aggregation of lignin chain connected with hydrophobic aromatic skeletons may accrue via the van der Waals attraction. [32]. SOFA using ESA cleaved more β-O-4 and β-β linkages, produced more G- lignin units, and thus decreased the S/G ratio, all of which might enhance the formation of the densely packed core of LNPs (Figure 12). As for SOFA using ESH, it broke down more β-O-4 and β-5 linkages, enriched S- lignin units, and increased S/G ratio, all of which might produce the LNPs with the loosely packed core. The diameters of LNPs from different SOFAs fit into these mechanisms very well.

Second, the hydrogen bonding interaction and electrostatic repulsion may also play an important role in the stability of LNPs. As the planar phenol groups from lignin may be compactly associated in layer to form the core of LNPs, the increased total phenolic OH groups should enhance the stability of LNPs through forming the hydrogen bonding networks. SOFA using ESA increased total phenolic OH group content and further facilitated the formation the LNPs with small effective diameter and high stability. When LNPs are dispersed in water, the phenolic OH groups and

possible COOH groups could provide the particles with a surface charge and promote the formation of electrical double-layers to stabilize the LNPs dispersion [31]. SOFA using ESA and ESH enriched the total phenolic OH and COOH groups, and thus increased the zeta potential and improved the stability of LNPs (Figures 5 and 12). However, COOH group is a key factor affecting the hydrophilicity of lignin on the surface of LNPs. Higher COOH content may facilitate the fabrication of LNPs with bigger particle size due to the enhanced hydrophilicity of lignin. Therefore, LNPs produced from SOFA using ESH have bigger effective diameters than that using ESA.

Third, the condensation of aromatic groups in lignin occurred in SOFA using ESA, which potentially enhanced the hydrophobic self-assembly process of lignin, and thus enabled the LNP fabrication with small particle size [49]. Because the covalent carbon-carbon single bonds of condensed lignin were much stronger than the π-π and van der Waals interactions, the cores of LNPs formed from condensed lignin should be more compact, and the corresponding LNPs exhibited smaller particle size [32, 49].

Taken these together, due to the amphiphilic property of lignin molecules and their unique phase behaviors in selective solvents, spherical LNPs with more uniformity and stability were fabricated through tailoring the lignin chemistry by SOFA, such as increased molecular weight lignin, decreased S/G ratio, cleaved β-O-4 and β-β linkages, enriched phenolic OH and COOH groups, and enhanced the hydrophobicity. Considering their good uniformity and stability, the LNPs could be used in applications where a uniform distribution of the nanoparticles is required, for instance, in drug delivery, substrate modifiers, energy storage, wound healing, coating formulations, biocidal active substances, and slow release fertilizers [32, 59, 66]. Therefore, the fabrication of LNPs not only presents a potential approach to upgrading of lignin, but also opens new avenues for value-added applications of lignin-based products.

4 Conclusions

High-quality LNPs with a spherical shape, small effective diameter, and good stability have been successfully fabricated by tailoring lignin chemistry through SOFA. The smallest effective diameter was 130 nm obtained from SOFA using ESA at stage 1. The half-width, PDI, and zeta potential of these LNPs were less than 50 nm,

0.08, and -50 mV, respectively, suggesting the good uniformity and stability of LNPs. The diverse lignin chemistries from SOFA design enabled the fundamental studies of the impact of lignin characteristics on LNP formation and stability. SOFA using ESA reduced the S/G ratio, decreased the β-O-4 linkage, and exposed more phenolic OH groups, promoting the formation of uniform and stable LNPs. Additionally, the SOFA design optimized both carbohydrate output and high quality LNP production, enabling the more complete utilization of biomass for value-added products.

Competing interests

The authors declare that they have no competing interests

Acknowledgements

The work was financially supported by the U.S. DOE (Department of Energy) EERE (Energy Efficiency and Renewable Energy) BETO (Bioenergy Technology Office) (grant no. DE-EE0006112).

References

1. L. H. Chen, J. Z. Dou, Q. L. Ma, N. Li, R. C. Wu, H. Y. Bian, D. J. Yelle, T. Vuorinen, S. Y. Fu, X. J. Pan and J. Y. Zhu, *Sci Adv*, 2017, **3**.
2. D. R. Vardon, M. A. Franden, C. W. Johnson, E. M. Karp, M. T. Guarnieri, J. G. Linger, M. J. Salm, T. J. Strathmann and G. T. Beckham, *Energ Environ Sci*, 2015, **8**, 617-628.
3. R. Rinaldi, R. Jastrzebski, M. T. Clough, J. Ralph, M. Kennema, P. C. A. Bruijnincx and B. M. Weckhuysen, *Angew Chem Int Edit*, 2016, **55**, 8164-8215.
4. T. Renders, S. Van den Bosch, S. F. Koelewijn, W. Schutyser and B. F. Sels, *Energ Environ Sci*, 2017, **10**, 1551-1557.
5. F. Xu, J. Sun, N. V. S. N. M. Konda, J. Shi, T. Dutta, C. D. Scown, B. A. Simmons and S. Singh, *Energ Environ Sci*, 2016, **9**, 1042-1049.
6. H. Z. Chen and Z. H. Liu, *Eng Life Sci*, 2017, **17**, 489-499.
7. Z. Chen and C. X. Wan, *Renew Sust Energ Rev*, 2017, **73**, 610-621.
8. Z. H. Liu, S. X. Xie, F. R. Lin, M. J. Jin and J. S. Yuan, *Biotechnol Biofuels*, 2018, **11**.
9. W. Schutyser, T. Renders, S. Van den Bosch, S. F. Koelewijn, G. T. Beckham and B. F. Sels, *Chem Soc Rev*, 2018, **47**, 852-908.
10. M. De Bruyn, J. Fan, V. L. Budarin, D. J. Macquarrie, L. D. Gomez, R. Simister, T. J. Farmer, W. D. Raverty, S. J. McQueen-Mason and J. H. Clark, *Energ Environ Sci*, 2016, **9**, 2571-2574.
11. S. Gillet, M. Aguedo, L. Petitjean, A. R. C. Morais, A. M. D. Lopes, R. M. Lukasik and P. T. Anastas, *Green Chem*, 2017, **19**, 4200-4233.
12. S. D. Shinde, X. Z. Meng, R. Kumar and A. J. Ragauskas, *Green Chem*, 2018, **20**, 2192-2205.
13. W. Boerjan, J. Ralph and M. Baucher, *Annu Rev Plant Biol*, 2003, **54**, 519-546.
14. H. Luo and M. M. Abu-Omar, *Green Chem*, 2018, **20**, 745-753.
15. L. A. Donaldson, *Phytochemistry*, 2001, **57**, 859-873.

16. J. Zakzeski, P. C. A. Bruijnincx, A. L. Jongerius and B. M. Weckhuysen, *Chem Rev*, 2010, **110**, 3552-3599.
17. M. R. Roussel and C. Lim, *Macromolecules*, 1995, **28**, 370-376.
18. M. E. Himmel, S. Y. Ding, D. K. Johnson, W. S. Adney, M. R. Nimlos, J. W. Brady and T. D. Foust, *Science*, 2007, **315**, 804-807.
19. G. T. Beckham, C. W. Johnson, E. M. Karp, D. Salvachua and D. R. Vardon, *Curr Opin Biotech*, 2016, **42**, 40-53.
20. A. J. Ragauskas, G. T. Beckham, M. J. Biddy, R. Chandra, F. Chen, M. F. Davis, B. H. Davison, R. A. Dixon, P. Gilna, M. Keller, P. Langan, A. K. Naskar, J. N. Saddler, T. J. Tschaplinski, G. A. Tuskan and C. E. Wyman, *Science*, 2014, **344**, 709-+.
21. D. M. Alonso, S. H. Hakim, S. F. Zhou, W. Y. Won, O. Hosseinaei, J. M. Tao, V. Garcia-Negron, A. H. Motagamwala, M. A. Mellmer, K. F. Huang, C. J. Houtman, N. Labbe, D. P. Harper, C. T. Maravelias, T. Runge and J. A. Dumesic, *Sci Adv*, 2017, **3**.
22. E. M. Karp, T. R. Eaton, V. S. I. Nogue, V. Vorotnikov, M. J. Biddy, E. C. D. Tan, D. G. Brandner, R. M. Cywar, R. M. Liu, L. P. Manker, W. E. Michener, M. Gilhespy, Z. Skoufa, M. J. Watson, O. S. Fruchey, D. R. Vardon, R. T. Gill, A. D. Bratis and G. T. Beckham, *Science*, 2017, **358**, 1307-1310.
23. M. Oliet, F. Rodriguez, A. Santos, M. A. Gilarranz, F. Garcia-Ochoa and J. Tijero, *Ind Eng Chem Res*, 2000, **39**, 34-39.
24. S. Van den Bosch, W. Schutyser, R. Vanholme, T. Driessen, S. F. Koelewijn, T. Renders, B. De Meester, W. J. J. Huijgen, W. Dehaen, C. M. Courtin, B. Lagrain, W. Boerjan and B. F. Sels, *Energ Environ Sci*, 2015, **8**, 1748-1763.
25. X. B. Zhao, S. M. Li, R. C. Wu and D. H. Liu, *Biofuel Bioprod Bior*, 2017, **11**, 567-590.
26. C. Wang, H. Li, M. Li, J. Bian and R. Sun, *Scientific reports*, 2017, **7**, 593.
27. T. Walser, L. K. Limbach, R. Brogioli, E. Erismann, L. Flamigni, B. Hattendorf, M. Juchli, F. Krumeich, C. Ludwig, K. Prikopsky, M. Rossier, D. Saner, A. Sigg, S. Hellweg, D. Gunther and W. J. Stark, *Nat Nanotechnol*, 2012, **7**, 520-524.
28. A. P. Richter, B. Bharti, H. B. Armstrong, J. S. Brown, D. Plemmons, V. N. Paunov, S. D. Stoyanov and O. D. Velev, *Langmuir : the ACS journal of surfaces and colloids*, 2016, **32**, 6468-6477.
29. R. P. Overend and E. Chornet, *Philos T R Soc A*, 1987, **321**, 523-536.
30. M. Pedersen and A. S. Meyer, *New Biotechnol*, 2010, **27**, 739-750.
31. M. Lievonen, J. J. Valle-Delgado, M. L. Mattinen, E. L. Hult, K. Lintinen, M. A. Kostiainen, A. Paananen, G. R. Szilvay, H. Setala and M. Osterberg, *Green Chem*, 2016, **18**, 1416-1422.
32. Y. Qian, Y. H. Deng, X. Q. Qiu, H. Li and D. J. Yang, *Green Chem*, 2014, **16**, 2156-2163.
33. C. G. Yoo, M. Li, X. Z. Meng, Y. Q. Pu and A. J. Ragauskas, *Green Chem*, 2017, **19**, 2006-2016.
34. Y. Q. Pu, S. L. Cao and A. J. Ragauskas, *Energ Environ Sci*, 2011, **4**, 3154-3166.
35. C. N. Hamelinck, G. van Hooijdonk and A. P. C. Faaij, *Biomass Bioenerg*, 2005, **28**, 384-410.
36. J. He and W. N. Zhang, *Appl Energ*, 2011, **88**, 1224-1232.
37. L. Qin, Z. H. Liu, B. Z. Li, B. E. Dale and Y. J. Yuan, *Bioresour. Technol.*, 2012, **112**, 319-326.
38. X. Z. Meng, T. Wells, Q. N. Sun, F. Huang and A. Ragauskas, *Green Chem*, 2015, **17**, 4239-4246.
39. T. Y. Zhang, R. Kumar, Y. D. Tsai, R. T. Elander and C. E. Wyman, *Green Chem*, 2015, **17**,

394-403.
40. K. Karimi and M. J. Taherzadeh, *Bioresource Technology*, 2016, **203**, 348-356.
41. S. D. Shinde, X. Meng, R. Kumar and A. J. Ragauskas, *Green Chem*, 2018, DOI: 10.1039/C8GC00353J.
42. J. Fernandez-Rodriguez, X. Erdocia, C. Sanchez, M. G. Alriols and J. Labidi, *J Energy Chem*, 2017, **26**, 622-631.
43. B. S. Donohoe, S. R. Decker, M. P. Tucker, M. E. Himmel and T. B. Vinzant, *Biotechnol Bioeng*, 2008, **101**, 913-925.
44. P. Alvira, E. Tomas-Pejo, M. Ballesteros and M. J. Negro, *Bioresource Technology*, 2010, **101**, 4851-4861.
45. T. Renders, S. Van den Bosch, T. Vangeel, T. Ennaert, S. F. Koelewijn, G. Van den Bossche, C. M. Courtin, W. Schutyser and B. F. Sels, *Acs Sustain Chem Eng*, 2016, **4**, 6894-6904.
46. C. Z. Li, X. C. Zhao, A. Q. Wang, G. W. Huber and T. Zhang, *Chem Rev*, 2015, **115**, 11559-11624.
47. H. Z. Chen and Z. H. Liu, *Biotechnol J*, 2015, **10**, 866-885.
48. H. Y. Bian, L. H. Chen, R. Gleisner, H. Q. Dai and J. Y. Zhu, *Green Chem*, 2017, **19**, 3370-3379.
49. D. Tian, J. G. Hu, R. P. Chandra, J. N. Saddler and C. H. Lu, *Acs Sustain Chem Eng*, 2017, **5**, 2702-2710.
50. C. Frangville, M. Rutkevicius, A. P. Richter, O. D. Velev, S. D. Stoyanov and V. N. Paunov, *Chemphyschem*, 2012, **13**, 4235-4243.
51. D. J. Dong, A. L. Fricke, B. M. Moudgil and H. Johnson, *Tappi J*, 1996, **79**, 191-197.
52. Z. J. Wei, Y. Yang, R. Yang and C. Y. Wang, *Green Chem*, 2012, **14**, 3230-3236.
53. E. Liu, M. Li, L. Das, Y. Pu, T. Frazier, B. Zhao, M. Crocker, A. J. Ragauskas and J. Shi, *Acs Sustain Chem Eng*, 2018, DOI: 10.1021/acssuschemeng.8b00384.
54. J. Li, G. Henriksson and G. Gellerstedt, *Bioresour Technol*, 2007, **98**, 3061-3068.
55. R. El Hage, N. Brosse, L. Chrusciel, C. Sanchez, P. Sannigrahi and A. Ragauskas, *Polym Degrad Stabil*, 2009, **94**, 1632-1638.
56. R. Samuel, Y. Q. Pu, B. Raman and A. J. Ragauskas, *Appl Biochem Biotech*, 2010, **162**, 62-74.
57. V. E. Tarabanko, D. V. Petukhov and G. E. Selyutin, *Kinet Catal+*, 2004, **45**, 569-577.
58. R. H. Narron, H. Kim, H. M. Chang, H. Jameel and S. Park, *Curr Opin Biotech*, 2016, **38**, 39-46.
59. I. A. Gilca, R. E. Ghitescu, A. C. Puitel and V. I. Popa, *Iran Polym J*, 2014, **23**, 355-363.
60. S. L. Cao, Y. Q. Pu, M. Studer, C. Wyman and A. J. Ragauskas, *Rsc Adv*, 2012, **2**, 10925-10936.
61. P. Sannigrahi, A. J. Ragauskas and S. J. Miller, *Energ Fuel*, 2010, **24**, 683-689.
62. P. Sannigrahi, A. J. Ragauskas and S. J. Miller, *Bioenerg Res*, 2008, **1**, 205-214.
63. G. Moxley, A. R. Gaspar, D. Higgins and H. Xu, *J. Ind. Microbiol. Biotechnol.*, 2012, **39**, 1289-1299.
64. A. Jensen, Y. Cabrera, C. W. Hsieh, J. Nielsen, J. Ralph and C. Felby, *Holzforschung*, 2017, **71**, 461-469.
65. L. Zhang, H. Shen and A. Eisenberg, *Macromolecules*, 1997, **30**, 1001-1011.
66. D. Kai, M. J. Tan, P. L. Chee, Y. K. Chua, Y. L. Yap and X. J. Loh, *Green Chem*, 2016, **18**, 1175-1200.

Figure captions

Figure 1 Schematic process of sequential organosolv fragmentation approach (SOFA) using low holding temperature for releasing fermentable sugar and fragmenting lignin polymer into soluble lignin streams

Figure 2 Fermentable sugar yields in the whole fractionation process by sequential organosolv fragmentation approach (SOFA). Fragmentation approaches are described in Table 1. ESA stands for ethanol plus sulfuric acid; EFA stands for ethanol plus formic acid; ESH stands for ethanol plus sodium hydroxide. S1, S2 and S3 stand for stage 1, stage 2 and stage 3, respectively

Figure 3 The lignin distributions in the solid and liquid streams after each SOFA. Fragmentation approaches are described in Table 1. ESA stands for ethanol plus sulfuric acid; EFA stands for ethanol plus formic acid; ESH stands for ethanol plus sodium hydroxide. S1, S2 and S3 stand for stage 1, stage 2 and stage 3, respectively.

Figure 4 Particle size distribution of lignin nanoparticles (LNPs) fabricated by self-assembly of lignin fractionated from sequential organosolv fragmentation approach (SOFA). ESA stands for ethanol with sulfuric acid; ESH stands for ethanol with sodium hydroxide. S1, S2 and S3 stand for stage 1, stage 2 and stage 3, respectively.

Figure 5 The properties of LNPs fabricated from the lignin fractionated by sequential organosolv fragmentation approach (SOFA), and their stability at different time periods. ESA stands for ethanol with sulfuric acid; ESH stands for ethanol with sodium hydroxide. S1, S2 and S3 stand for stage 1, stage 2 and stage 3, respectively

Figure 6 Stability of lignin nanoparticles (LNPs) fabricated from fractionated lignin by each sequential organosolv fragmentation approach (SOFA) at different pH values. ESA stands for ethanol with sulfuric acid; ESH stands for ethanol with sodium hydroxide. S1, S2 and S3 stand for stage 1, stage 2 and stage 3, respectively.

Figure 7 Stability of lignin nanoparticles (LNPs) fabricated from fractionated lignin by each sequential organosolv fragmentation approach (SOFA) at different NaCl concentrations. ESA stands for ethanol with sulfuric acid; ESH stands for ethanol with sodium hydroxide. S1, S2 and S3 stand for stage 1, stage 2 and stage 3, respectively.

Figure 8 Molecular weight distributions of the corn stover native lignin (CSNL) and fractionated lignin produced by sequential organosolv fragmentation approach (SOFA). Pretreatment strategies are described in Table 1. ESA stands for ethanol with sulfuric acid; EFA stands for ethanol with formic acid; ESH stands for ethanol with sodium hydroxide. S1, S2 and S3 stand for stage 1, stage 2 and stage 3, respectively.

Figure 9 Semi-quantitative information on lignin subunits in fractionated lignin produced after sequential organosolv fragmentation approach (SOFA) as detected using 2D HSQC NMR. ESA stands for ethanol plus sulfuric acid; EFA stands for ethanol plus formic acid; ESH stands for ethanol plus sodium hydroxide. S1, S2 and S3 stand for stage 1, stage 2 and stage 3, respectively.

Figure 10 Semi-quantitative information on lignin interunit linkages in corn stover native lignin (CSNL) and fractionated lignin produced after sequential organosolv fragmentation approach (SOFA) as detected using 2D HSQC NMR. ESA stands for ethanol plus sulfuric acid; EFA stands for ethanol plus formic acid; ESH stands for ethanol plus sodium hydroxide. S1, S2 and S3 stand for stage 1, stage 2 and stage 3, respectively.

Figure 11 Contents of hydroxyl groups in the fractionated lignins produced by sequential organosolv fragmentation approach (SOFA) as detected using ^{31}P NMR. ESA stands for ethanol plus sulfuric acid;

EFA stands for ethanol plus formic acid; ESH stands for ethanol plus sodium hydroxide. S1, S2 and S3 stand for stage 1, stage 2 and stage 3, respectively

Figure 12 Correlations of the effective diameter of lignin nanoparticles (LNPs) with tailored lignin chemistry by sequential organosolv fragmentation approach (SOFA). Mw represents weight-average molecular weight, g/mol; Mn represents number-average molecular weight, g/mol; PDI represents polydispersity index; ESA represents ethanol plus sulfuric acid; ESH represents ethanol plus sodium hydroxide. S1, S2 and S3 represent stage 1, stage 2 and stage 3, respectively.

Table 1 Sequential organosolv fragmentation approach (SOFA) using low holding temperature for tailoring the lignin reactivity towards its high-value utilization from corn stover biomass

Experiment No.			Stage 1		Stage 2		Stage 3	
	Chemicals	**Initial pH**	**Conditions**	**logR_0"**	**Conditions**	**logR_0"**	**Conditions**	**logR_0"**
SOFA 1	50% ethanol+1% Sulfuric acid	1.8	120 ˚C, 15 min	7.0	120 ˚C, 30 min	7.3	120 ˚C, 60 min	7.6
SOFA 2	50% ethanol+2% Formic acid	3.8	120 ˚C, 15 min	5.0	120 ˚C, 30 min	5.3	120 ˚C, 60 min	5.6
SOFA 3	50% ethanol	6.2	120 ˚C, 15 min	2.7	120 ˚C, 30 min	2.9	120 ˚C, 60 min	3.2
SOFA 4	50% ethanol+1% Sodium hydroxide	13.0	120 ˚C, 15 min	7.8	120 ˚C, 30 min	8.1	120 ˚C, 60 min	8.4

S1, S2 and S3 represent Stage 1, Stage 2, and Stage 3, respectively; % is based on the weight percent, w/w; log R_0" is calculated based on Equation 2

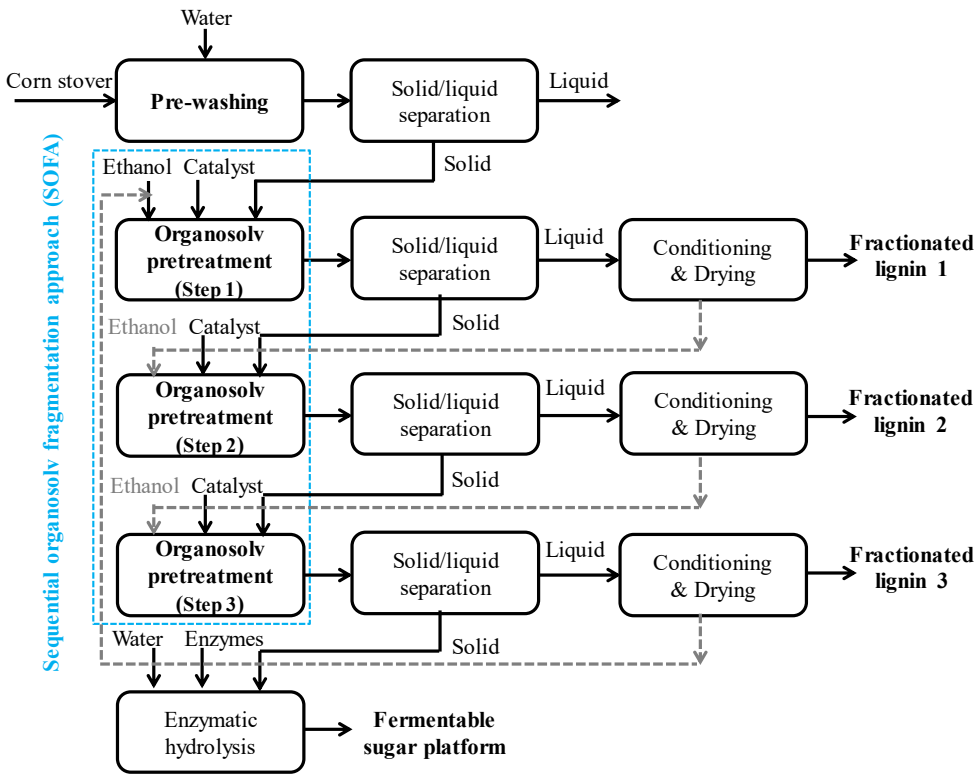

Figure 1 Schematic process of sequential organosolv fragmentation approach (SOFA) using low holding temperature for releasing fermentable sugar and fragmenting lignin polymer into soluble lignin streams

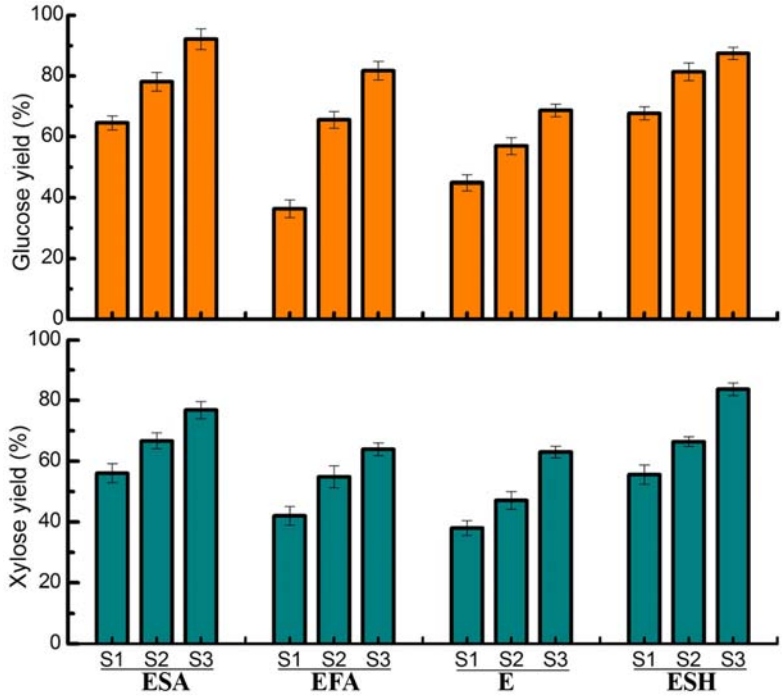

Figure 2 Fermentable sugar yields in the whole fractionation process by sequential organosolv fragmentation approach (SOFA). Fragmentation approaches are described in Table 1. ESA represents ethanol plus sulfuric acid; EFA represents ethanol plus formic acid; ESH represents ethanol plus sodium hydroxide. S1, S2 and S3 represent stage 1, stage 2 and stage 3, respectively.

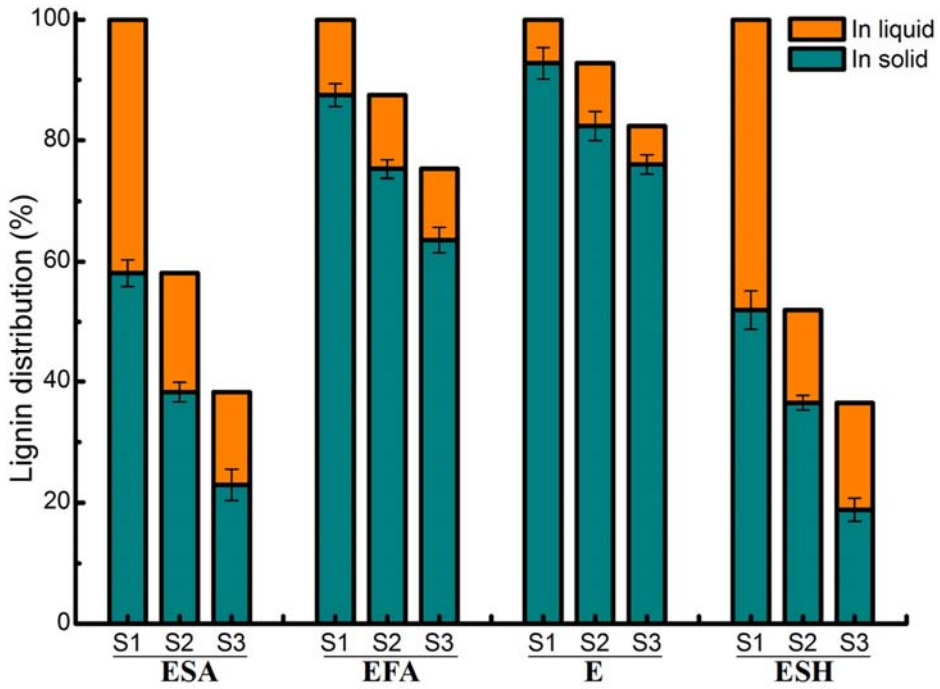

Figure 3 The lignin distributions in the solid and liquid streams after each SOFA. Fragmentation approaches are described in Table 1. ESA represents ethanol plus sulfuric acid; EFA represents ethanol plus formic acid; ESH represents ethanol plus sodium hydroxide. S1, S2 and S3 represent stage 1, stage 2 and stage 3, respectively

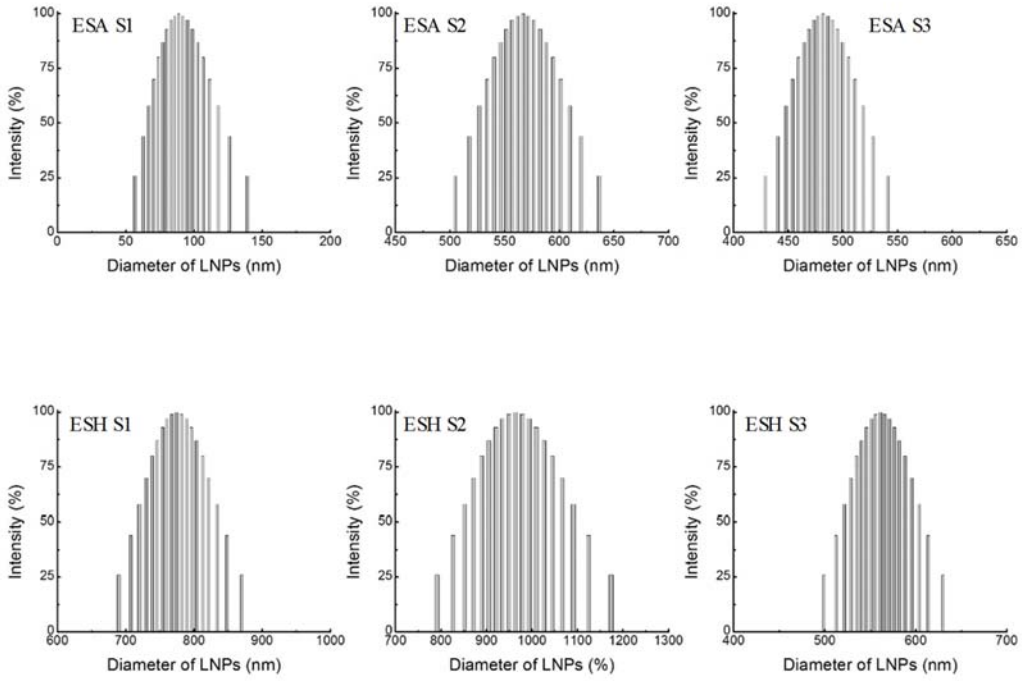

Figure 4 Particle size distributions of lignin nanoparticles (LNPs) fabricated by self-assembly of lignin fractionated from sequential organosolv fragmentation approach (SOFA). ESA represents ethanol with sulfuric acid; ESH represents ethanol with sodium hydroxide. S1, S2 and S3 represent stage 1, stage 2 and stage 3, respectively

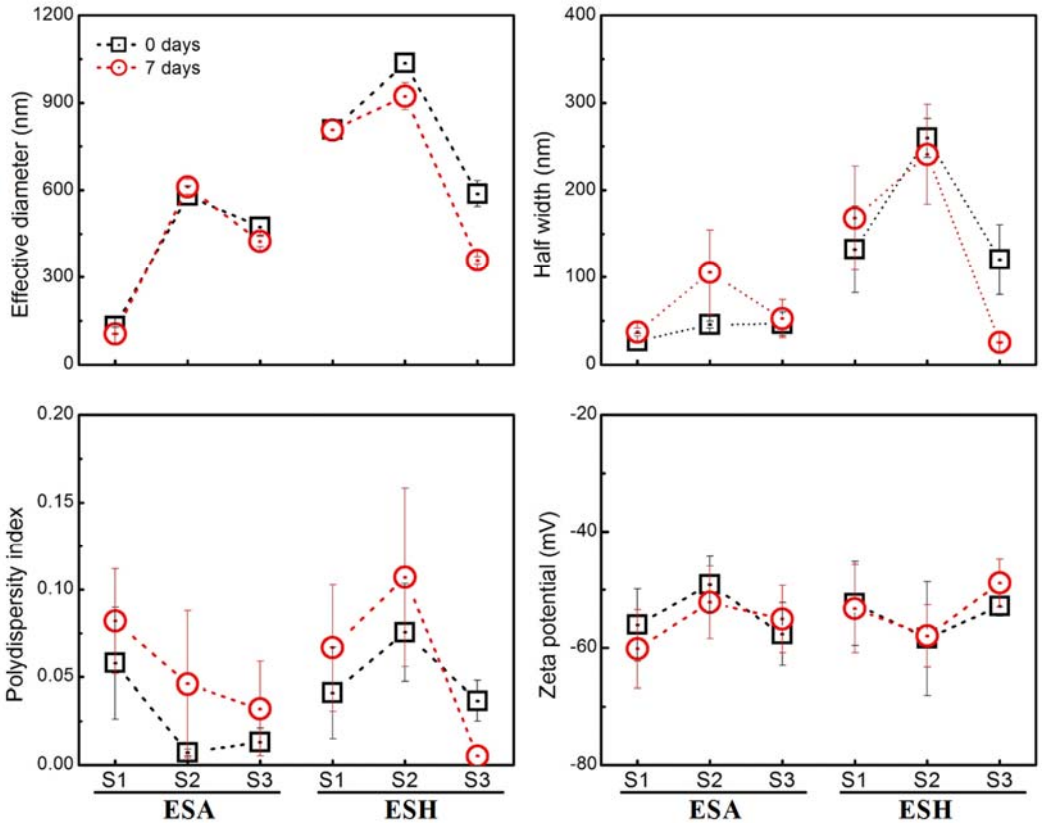

Figure 5 The property of LNPs fabricated from the lignin fractionated by sequential organosolv fragmentation approach (SOFA), and their stability at different time periods. ESA represents ethanol with sulfuric acid; ESH represents ethanol with sodium hydroxide. S1, S2 and S3 represent stage 1, stage 2 and stage 3, respectively.

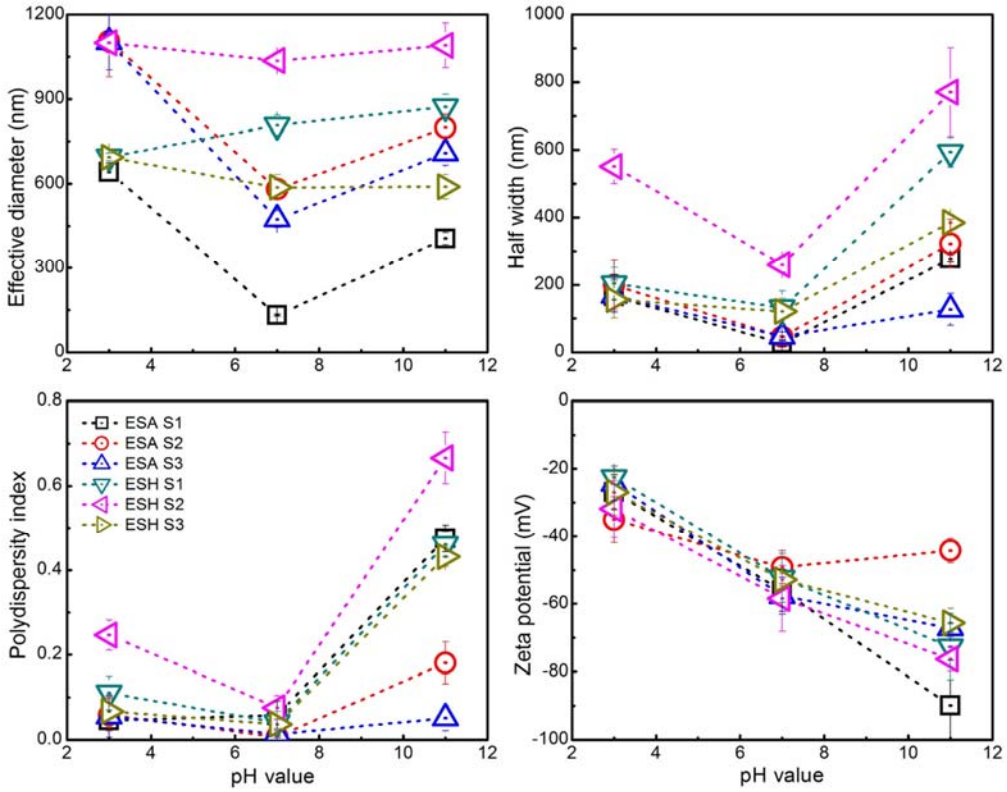

Figure 6 Stability of lignin nanoparticles (LNPs) fabricated from fractionated lignin by each sequential organosolv fragmentation approach (SOFA) at different pH values. ESA represents ethanol with sulfuric acid; ESH represents ethanol with sodium hydroxide. S1, S2 and S3 represent stage 1, stage 2 and stage 3, respectively.

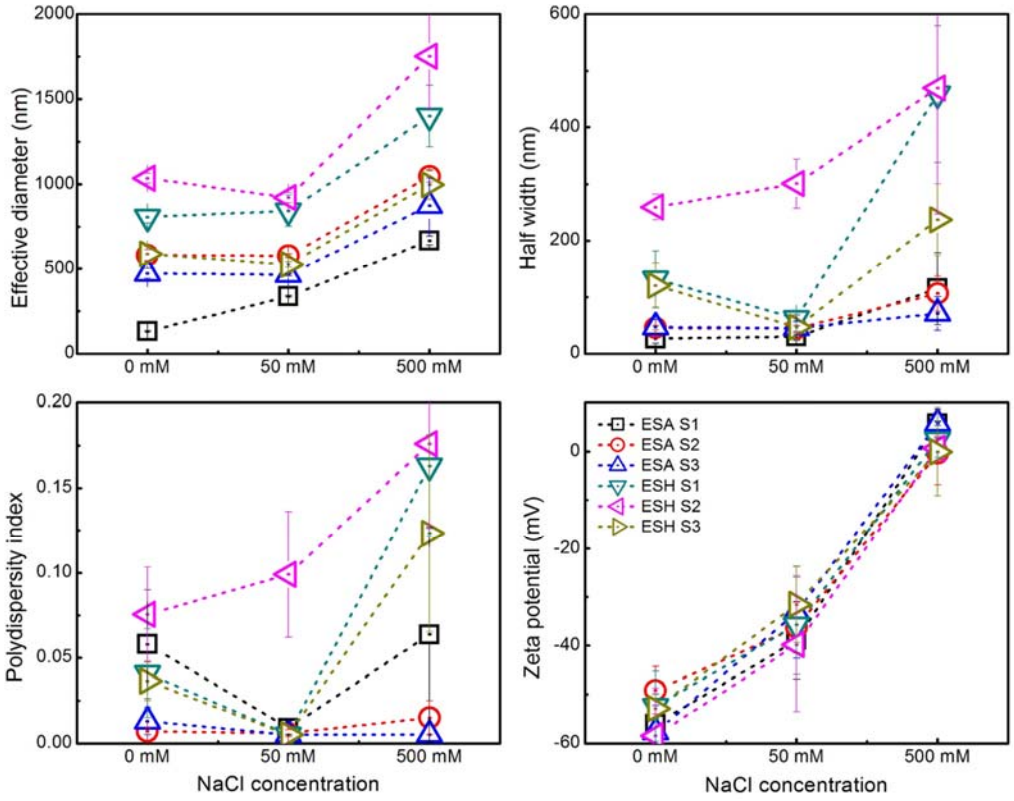

Figure 7 Stability of lignin nanoparticles (LNPs) fabricated from fractionated lignin by each sequential organosolv fragmentation approach (SOFA) at different NaCl concentrations. ESA represents ethanol with sulfuric acid; ESH represents ethanol with sodium hydroxide. S1, S2 and S3 represent stage 1, stage 2 and stage 3, respectively.

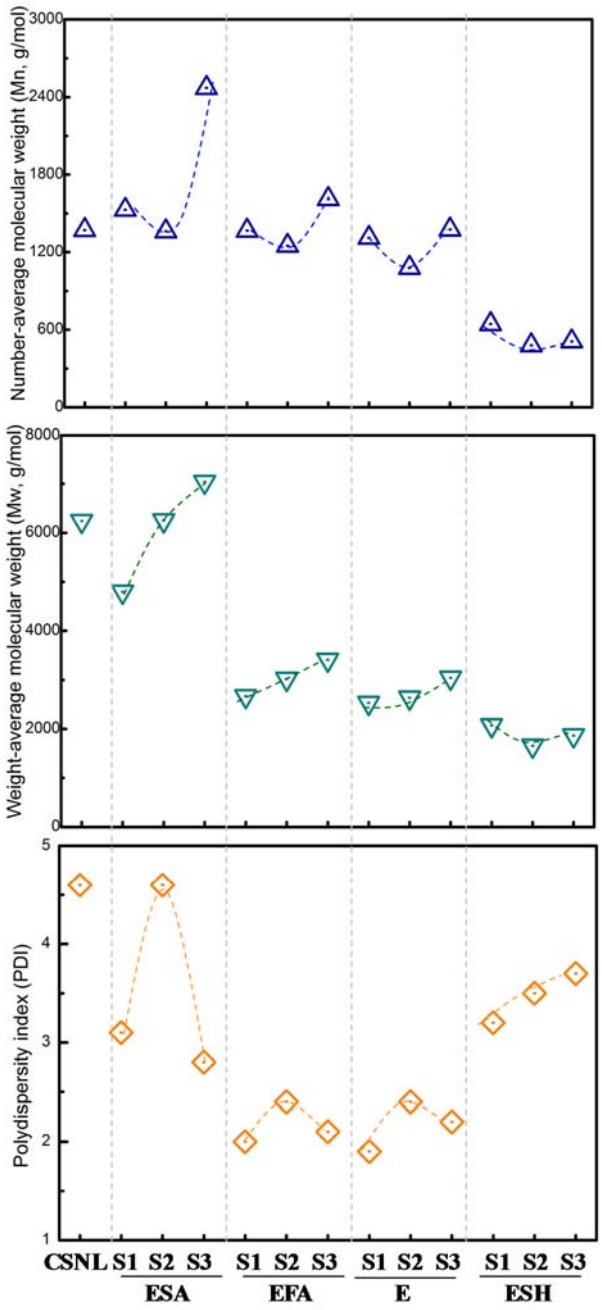

Figure 8 Molecular weight distributions of the corn stover native lignin (CSNL) and fractionated lignin produced by sequential organosolv fragmentation approach (SOFA). Pretreatment strategies are described in Table 1. ESA represents ethanol plus sulfuric acid; EFA represents ethanol plus formic acid; ESH represents ethanol plus sodium hydroxide. S1, S2 and S3 represent stage 1, stage 2 and stage 3, respectively

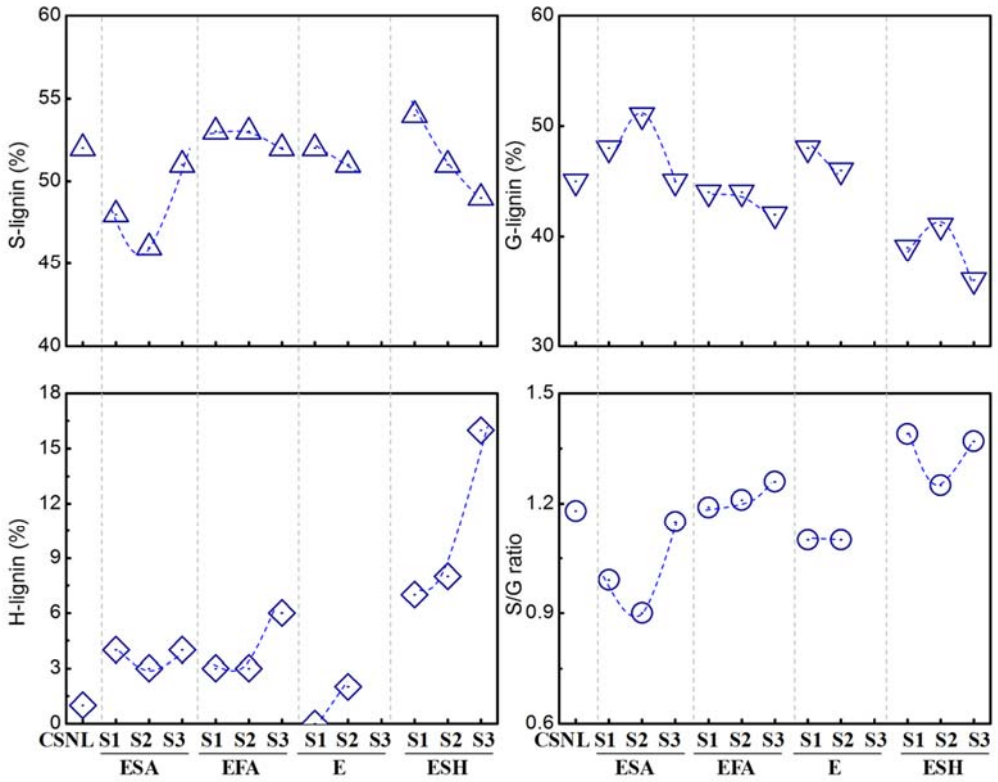

Figure 9 Semi-quantitative information on lignin subunits in fractionated lignin produced after sequential organosolv fragmentation approach (SOFA) as detected using 2D HSQC NMR. ESA represents ethanol plus sulfuric acid; EFA represents ethanol plus formic acid; ESH represents ethanol plus sodium hydroxide. S1, S2 and S3 represent stage 1, stage 2 and stage 3, respectively

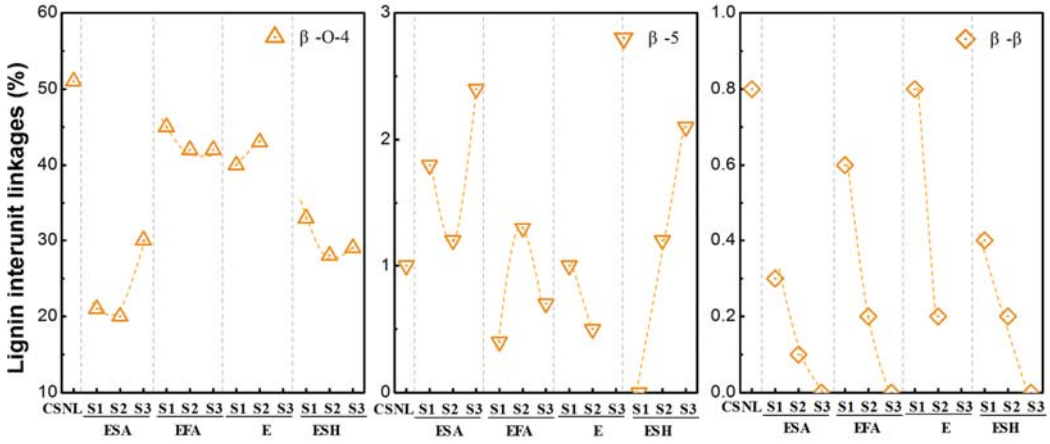

Figure 10 Semi-quantitative information on lignin interunit linkages in corn stover native lignin (CSNL) and fractionated lignin produced after sequential organosolv fragmentation approach (SOFA) as detected using 2D HSQC NMR. ESA represents ethanol plus sulfuric acid; EFA represents ethanol plus formic acid; ESH represents ethanol plus sodium hydroxide. S1, S2 and S3 represent stage 1, stage 2 and stage 3, respectively

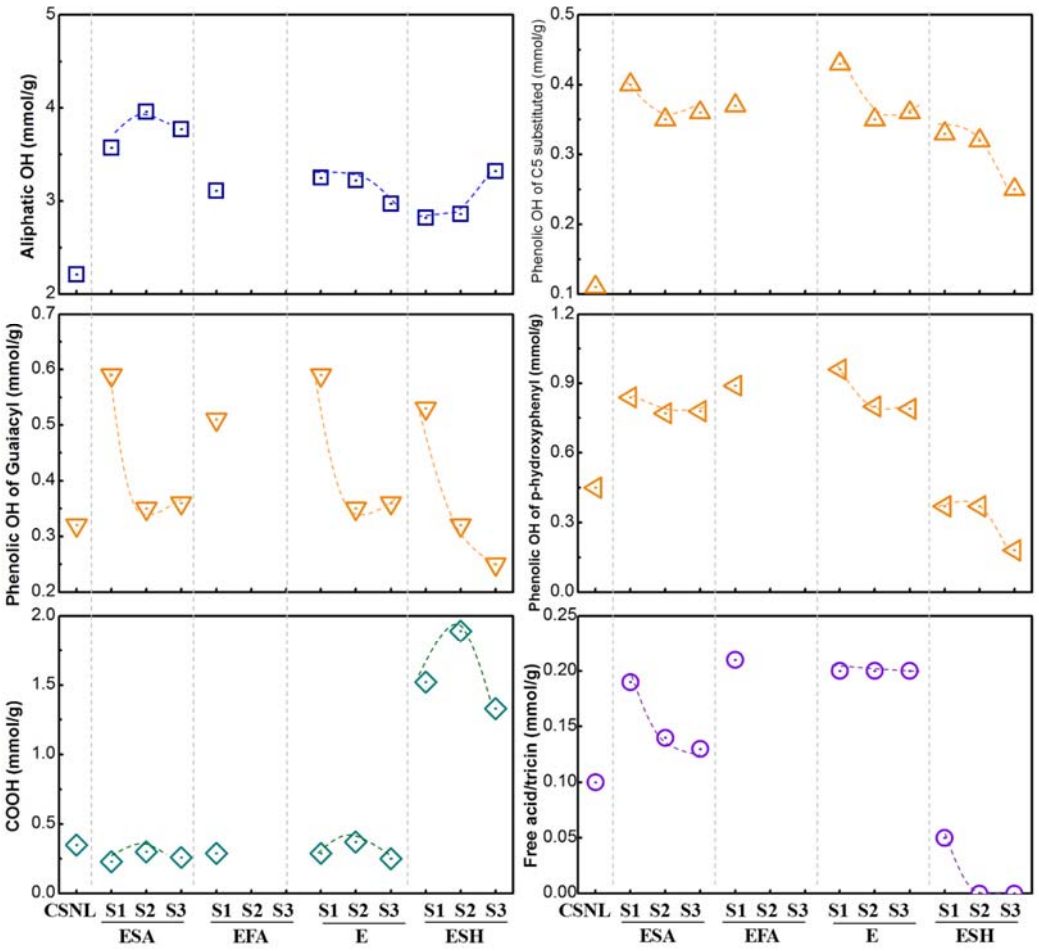

Figure 11 Contents of hydroxyl groups in the fractionated lignins produced by sequential organosolv fragmentation approach (SOFA) as detected using ^{31}P NMR. ESA represents ethanol plus sulfuric acid; EFA represents ethanol plus formic acid; ESH represents ethanol plus sodium hydroxide. S1, S2 and S3 represent stage 1, stage 2 and stage 3, respectively

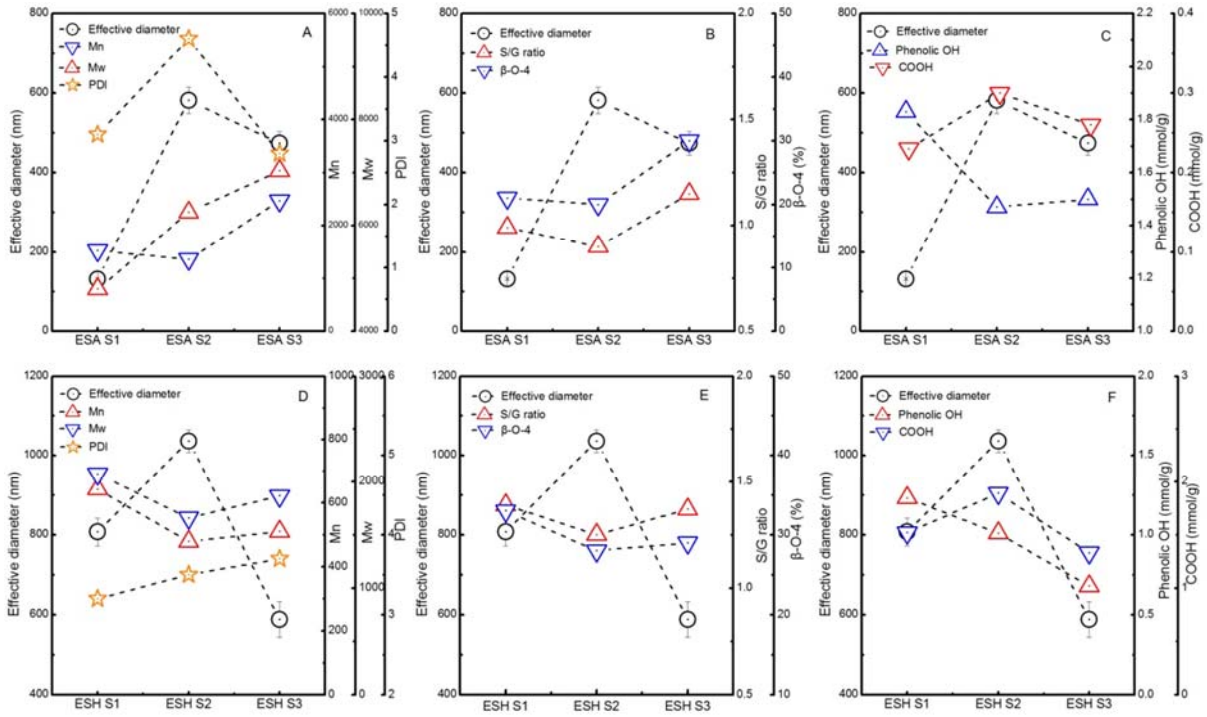

Figure 12 Correlations of the effective diameter of lignin nanoparticles (LNPs) with tailored lignin chemistry by sequential organosolv fragmentation approach (SOFA). Mw represents weight-average molecular weight, g/mol; Mn represents number-average molecular weight, g/mol; PDI represents polydispersity index; ESA represents ethanol plus sulfuric acid; ESH represents ethanol plus sodium hydroxide. S1, S2 and S3 represent stage 1, stage 2 and stage 3, respectively.

Electronic supplemental information A Component transformation in corn stover solid fraction by sequential organosolv fragmentation approach (SOFA). Fragmentation approaches were described in Table 1. CSFS stands for corn stover feedstock. ESA represents ethanol plus sulfuric acid; EFA represents ethanol plus formic acid; ESH represents ethanol plus sodium hydroxide. S1, S2 and S3 represent stage 1, stage 2 and stage 3, respectively

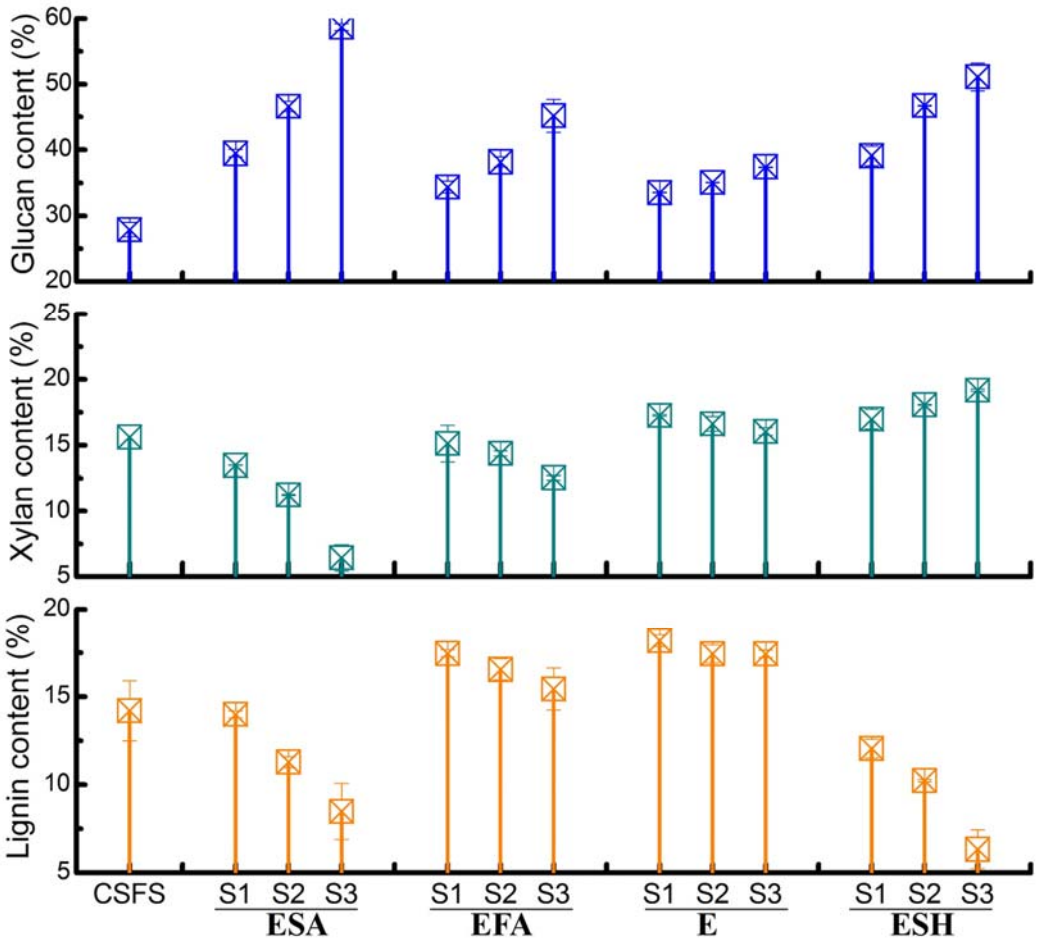

Electronic supplemental information B Enzymatic hydrolysis of pretreated solids by sequential organosolv fragmentation approach (SOFA). Fragmentation approaches are described in Table 1. CSFS stands for corn stover feedstock. ESA represents ethanol plus sulfuric acid; EFA represents ethanol plus formic acid; ESH represents ethanol plus sodium hydroxide. S1, S2 and S3 represent stage 1, stage 2 and stage 3, respectively

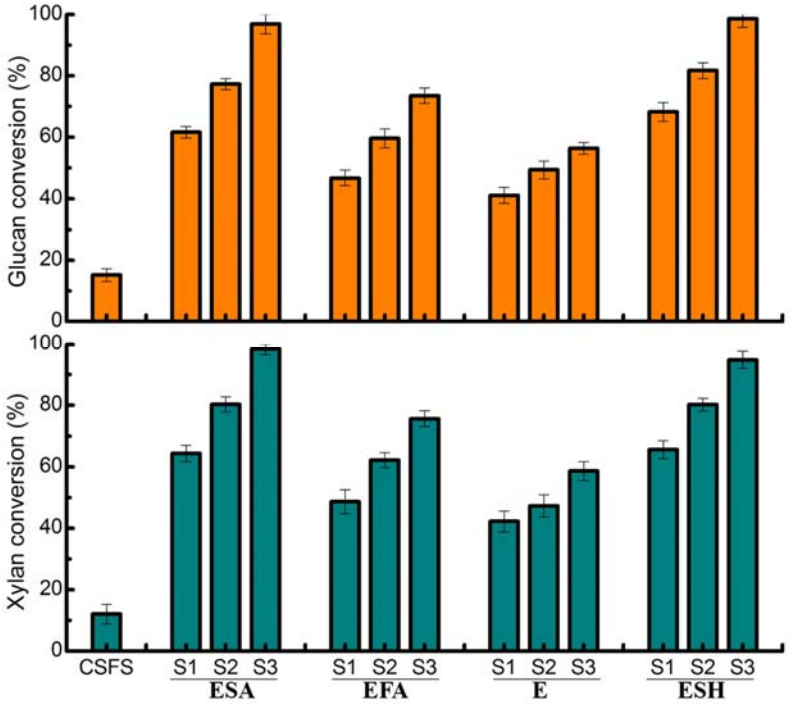

Electronic supplemental information C Correlations between the glucan/xylan conversion and removal rates of xylan and lignin. ESA represents ethanol plus sulfuric acid; EFA represents ethanol plus formic acid; ESH represents ethanol plus sodium hydroxide. S1, S2 and S3 represent stage 1, stage 2 and stage 3, respectively

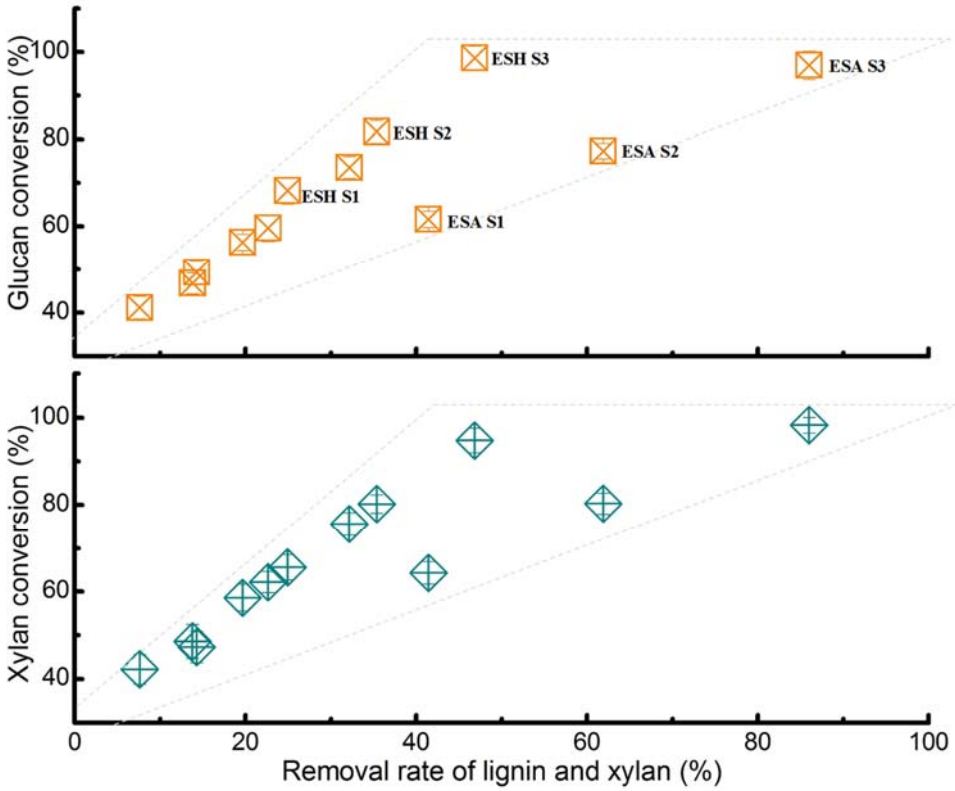

Electronic supplemental information D Mass balance of the whole sequential organosolv fragmentation approach (SOFA). A, SOFA using ethanol plus sulfuric acid (ESA); B, SOFA using ethanol plus sodium hydroxide (ESH). S1, S2 and S3 represent stage 1, 2 and 3, respectively

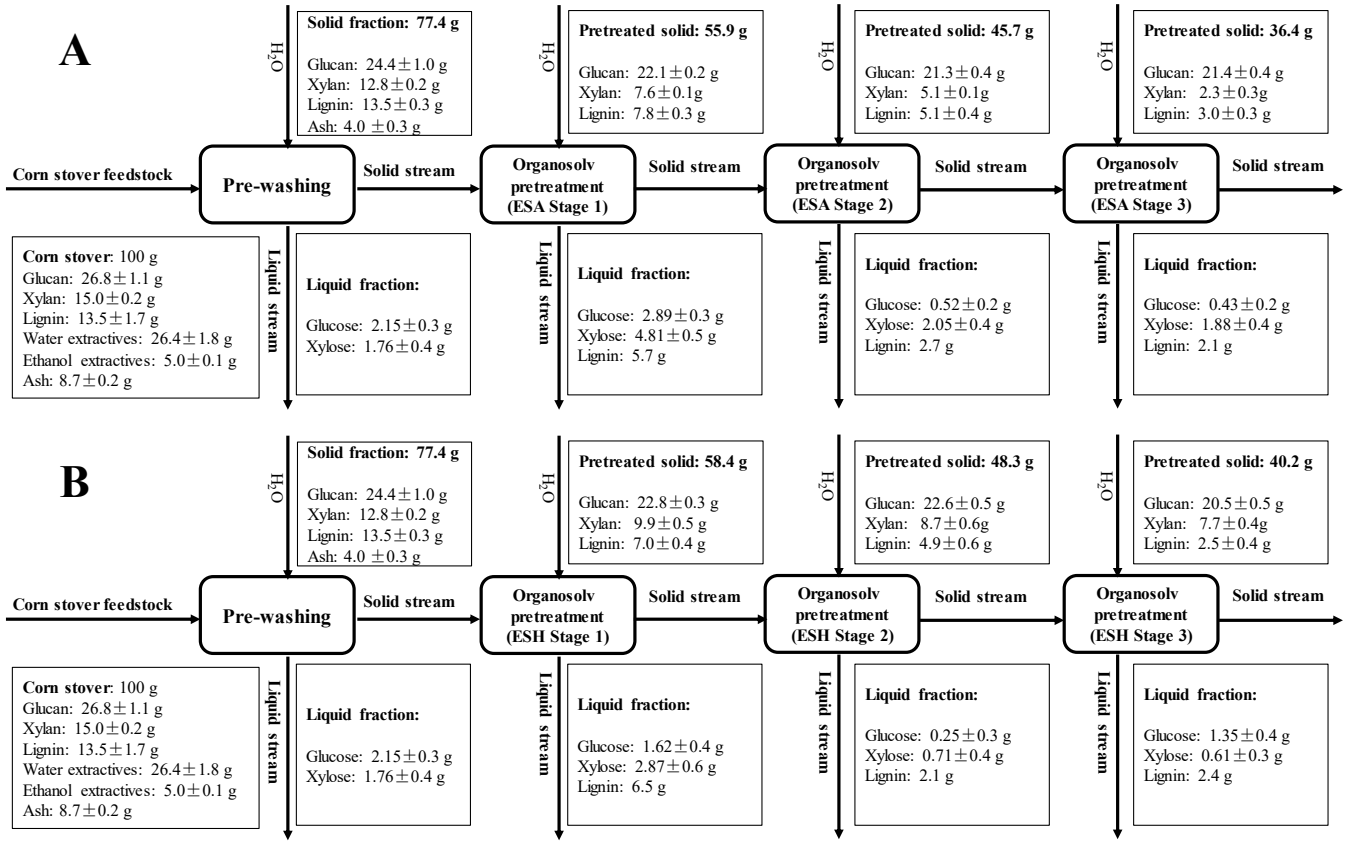

Electronic supplemental information E Scanning electron microscopy (SEM) (A, B, E, F) and scanning transmission electron microscopy (STEM) (C, D) images of lignin nanoparticles (LNPs) fabricated from lignin produced by sequential organosolv fragmentation approach (SOFA). ESA represents ethanol plus sulfuric acid; ESH represents ethanol plus sodium hydroxide. S1, S2 and S3 represent stage 1, stage 2 and stage 3, respectively

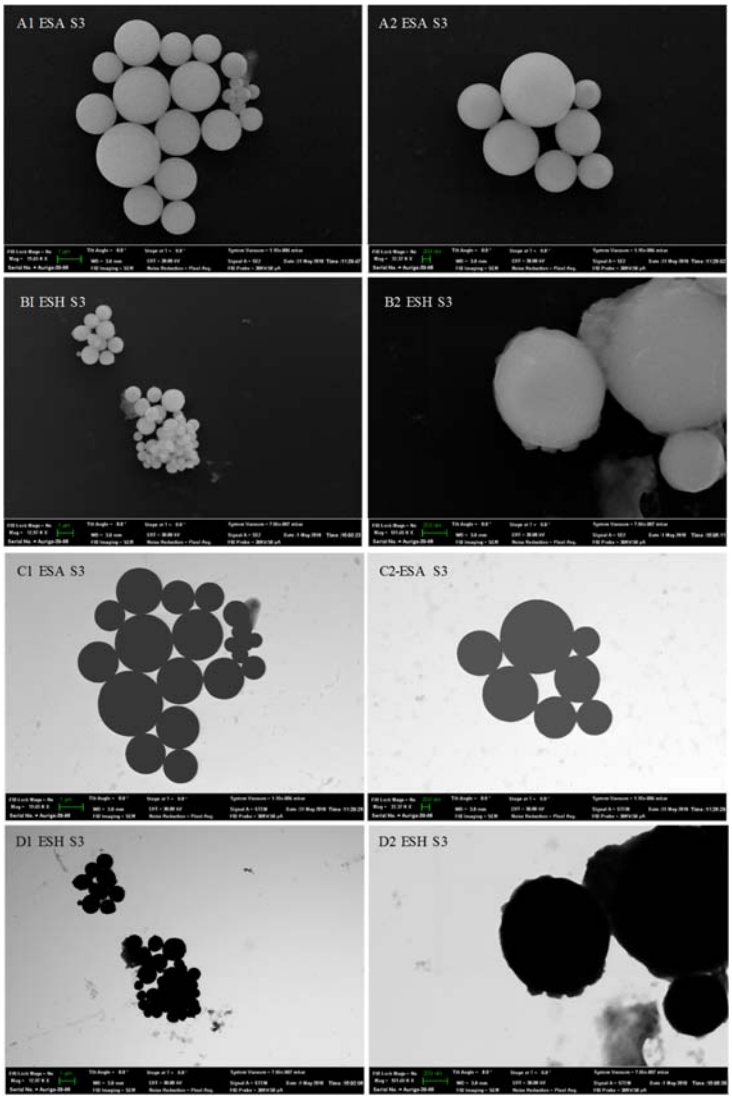

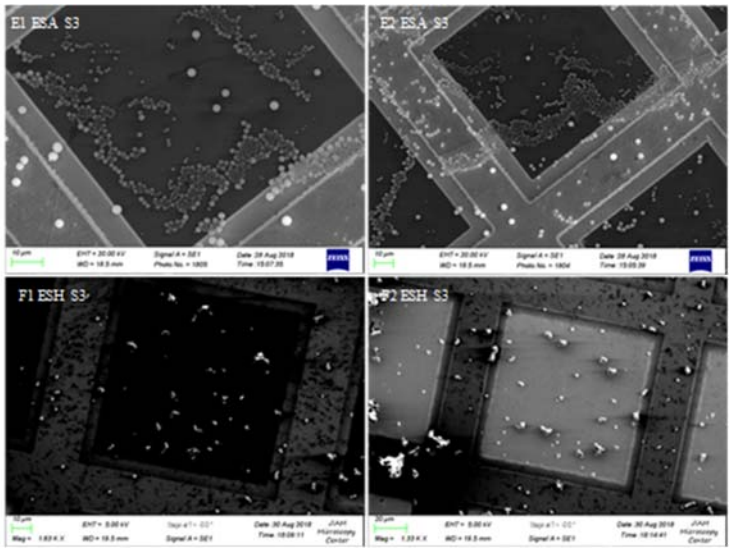
E1 ESA S3
E2 ESA S3
F1 ESH S3
F2 ESH S3

Electronic supplemental information F The yield of lignin nanoparticles (LNPs) fabricated from lignin produced at each stage of sequential organosolv fragmentation approach (SOFA). ESA represents ethanol plus sulfuric acid; ESH represents ethanol plus sodium hydroxide. S1, S2 and S3 represent stage 1, stage 2 and stage 3, respectively.

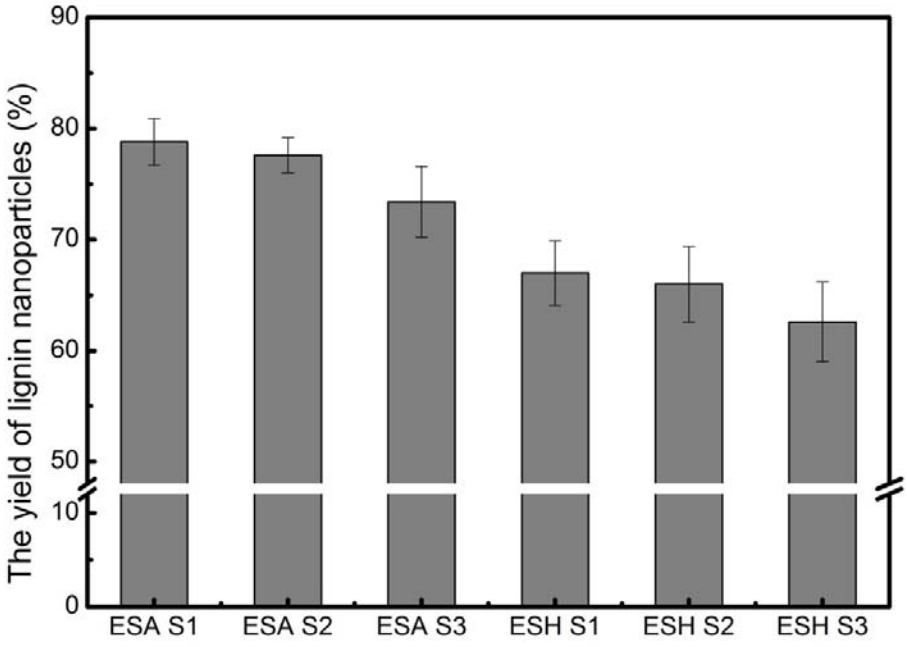

Electronic supplemental information G Aromatic and lignin interunit regions of 2D HSQC NMR spectra from the fractionated lignin produced from each sequential organosolv fragmentation approach (SOFA). ESA represents ethanol plus sulfuric acid; EFA represents ethanol plus formic acid; ESH represents ethanol plus sodium hydroxide. S1, S2 and S3 represent stage 1, stage 2 and stage 3, respectively

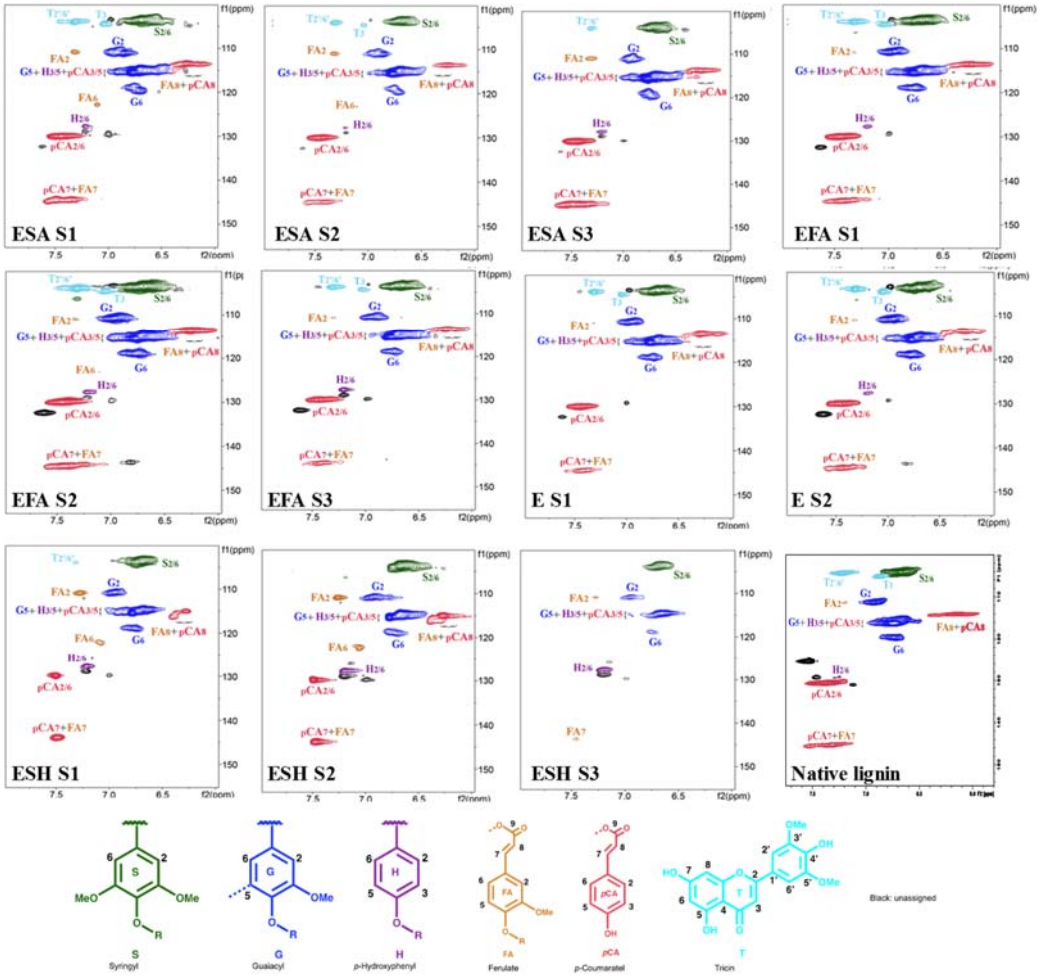

Electronic supplemental information H ^{31}P-NMR spectra of the fractionated lignin produced from each sequential organosolv fragmentation approach (SOFA). ESA represents ethanol plus sulfuric acid; EFA represents ethanol plus formic acid; ESH represents ethanol plus sodium hydroxide. S1, S2 and S3 represent stage 1, stage 2 and stage 3, respectively

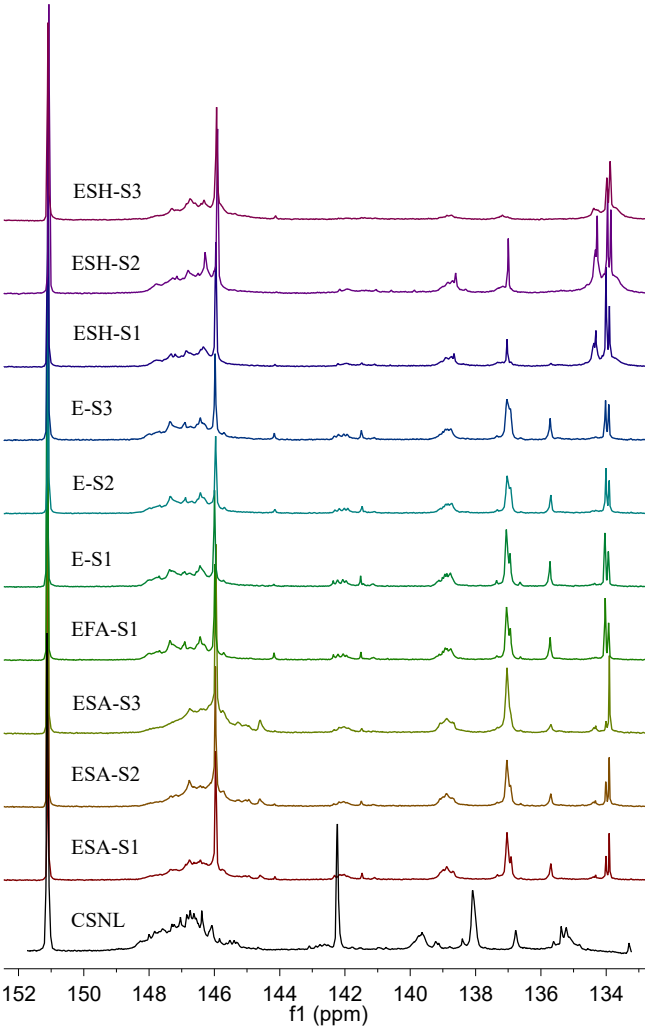

Electronic supplemental information I A proposed mechanism model of the self-assembly fabrication of lignin nanoparticles (LNPs) from corn stover lignin produced by sequential organosolv fragmentation approach (SOFA). ESA represents ethanol with sulfuric acid; ESH represents ethanol with sodium hydroxide. S1, S2 and S3 represent stage 1, stage 2 and stage 3, respectively. A-OH represents aliphatic hydroxyl group; P-OH represents phenolic hydroxyl group; CL represents condensed lignin; '+' represents an increase; and '-' represents a decrease.